Biochimica et Biophysica Acta 1777 (2008) 1229–1248

Contents lists available at ScienceDirect

Biochimica et Biophysica Acta

journal homepage: www.elsevier.com/locate/bbabio

Review

Coupling of electron transfer to proton uptake at the Q_B site of the bacterial reaction center: A perspective from FTIR difference spectroscopy

Eliane Nabedryk *, Jacques Breton

Service de Bioénergétique Biologie Structurale et Mécanismes, CEA-Saclay, 91191 Gif-sur-Yvette Cedex, France

ARTICLE INFO

Article history:
Received 23 April 2008
Received in revised form 26 June 2008
Accepted 27 June 2008
Available online 11 July 2008

Keywords:
FTIR
Reaction center
Quinone
Site-directed mutant
Carboxylic acid
Protonation event

ABSTRACT

FTIR difference spectroscopy provides a unique approach to study directly protonation/deprotonation events of carboxylic acids involved in the photochemical cycle of membrane proteins, such as the bacterial photosynthetic reaction center (RC). In this work, we review the data obtained by light-induced FTIR difference spectroscopy on the first electron transfer to the secondary quinone Q_B in native RCs and a series of mutant RCs. We first examine the approach of isotope-edited FTIR spectroscopy to investigate the binding site of Q_B. This method provides highly specific IR vibrational fingerprints of the bonding interactions of the carbonyls of Q_B and Q_B^- with the protein. The same isotope-edited IR fingerprints for the carbonyls of neutral Q_B have been observed for native *Rhodobacter sphaeroides* RCs and several mutant RCs at the Pro-L209, Ala-M260, or Glu-L212/Asp-L213 sites, for which X-ray crystallography has found the quinone in the proximal position. It is concluded that at room temperature Q_B occupies a single binding site that fits well the description of the proximal site derived from X-ray crystallography and that the conformational gate limiting the rate of the first electron transfer from $Q_A^-Q_B$ to $Q_AQ_B^-$ cannot be the movement of Q_B from its distal to proximal site. Possible alternative gating mechanisms are discussed. In a second part, we review the contribution of the various experimental measurements, theoretical calculations, and molecular dynamics simulations which have been actively conducted to propose which amino acid side chains near Q_B could be proton donors/acceptors. Further, we show how FTIR spectroscopy of mutant RCs has directly allowed several carboxylic acids involved in proton uptake upon first electron transfer to Q_B to be identified. Owing to the importance of a number of residues for high efficiency of coupled electron transfer reactions, the photoreduction of Q_B was studied in a series of single mutant RCs at Asp-L213, Asp-L210, Asp-M17, Glu-L212, Glu-H173, as well as combinations of these mutations in double and triple mutant RCs. The same protonation pattern was observed in the 1760–1700 cm^{-1} region of the Q_B^-/Q_B spectra of native and several mutant (DN-L213, DN-L210, DN-M17, EQ-H173) RCs. However, it was drastically modified in spectra of mutants lacking Glu at L212. The main conclusion of this work is that in native RCs from *Rb. sphaeroides*, Glu-L212 is the only carboxylic acid residue that contributes to proton uptake at all pH values (from pH 4 to pH 11) in response to the formation of Q_B^-. Another important result is that the residues Asp-L213, Asp-L210, Asp-M17, and Glu-H173 are mostly ionized in the Q_B state at neutral pH and do not significantly change their protonation state upon Q_B^- formation. In contrast, interchanging Asp and Glu at L212 and L213 (i.e., in the so-called swap mutant) led to the identification of a novel protonation pattern of carboxylic acids: at least four individual carboxylic acids were affected by Q_B reduction. The pH dependence of IR carboxylic signals in the swap mutant demonstrates that protonation of Glu-L213 occurred at pH > 5 whereas that of Asp-L212 occurred over the entire pH range from 8 to 4. In native RCs from *Rhodobacter sphaeroides*, a broad positive IR continuum around 2600 cm^{-1} in the Q_B^-/Q_B steady-state FTIR spectrum in ^1H_2O was assigned to delocalized proton(s) in a highly polarizable hydrogen-bonded network. The possible relation of the IR continuum band to the carboxylic acid residues and to bound water molecules involved in the proton transfer pathway was investigated by testing the robustness of this band to different mutations of acids. The presence of the band is not correlated with the localization of the proton on Glu-L212. The largest changes of the IR continuum were observed in single and double mutant RCs where Asp-L213 is not present. It is proposed that the changes observed in the mutant RCs with respect to native RCs reflect the specific role of bound protonated water molecule(s) located in the vicinity of Asp-L213 and undergoing hydrogen-bond changes in the network.

Abbreviations: P, primary electron donor; BChl, bacteriochlorophyll; Bphe, bacteriopheophytin; H_A, intermediate electron acceptor; Q_A, (Q_B), primary, (secondary), quinone electron acceptor; Q*n*, ubiquinone-*n*:, 2,3-dimethoxy-5-methyl-6-polyprenyl-1,4-benzoquinone; RC, reaction center; *Rb.*, *Rhodobacter*; *B.*, *Blastochloris*; ET, electron transfer; FTIR, Fourier transform infrared; RS, rapid-scan; TR, time-resolved; EPR, electron paramagnetic resonance; ENDOR, electron nuclear double resonance

* Corresponding author. Tel.: +33 1 69 08 71 12; fax: +33 1 69 08 87 17.
E-mail address: eliane.nabedryk@cea.fr (E. Nabedryk).

0005-2728/$ – see front matter © 2008 Elsevier B.V. All rights reserved.
doi:10.1016/j.bbabio.2008.06.012

1. Introduction

In bioenergetic systems, electron and proton transfer reactions are fundamental processes required for the generation and interconversion of energy. In photosynthetic bacteria, the initial steps of light energy conversion into chemical energy occur in a membrane bound pigment-protein complex called the photochemical reaction center (RC) which couples electron and proton transfer across the bacterial membrane . The RC complex (~100 kDa) is composed of three (L, M, and H) or four (including a cytochrome unit) polypeptide subunits. With the three-dimensional structure determined at ~2 Å resolution, the protein amenable to site-directed mutagenesis, and the possibility to trigger the electron transfer (ET) reactions by a short pulse of light, the RC represents an ideal system for the study of proton-coupled ET reactions.

In the native RC, light-induced ET is exclusively initiated via the active A-branch of cofactors from the primary electron donor P (a dimer of bacteriochlorophyll) through a series of electron acceptors (notably the bacteriopheophytin H_A) to the primary quinone (Q_A), and then to the loosely bound secondary quinone Q_B (Fig. 1A). In RCs from *Rhodobacter* (*Rb.*) *capsulatus* and *Rb. sphaeroides*, Q_A and Q_B are both ubiquinone-10 (Q_{10}). A second ET coupled with the uptake of two protons from the solution results in the formation of the quinol Q_BH_2 that is subsequently released from the Q_B binding site and replaced by another quinone from a pool contained in the membrane. This physiologically important reaction, i.e., the double reduction and protonation of Q_B, together with the oxidation of Q_BH_2 by the cytochrome bc_1 complex, further initiates the formation of the proton gradient required for ATP synthesis [1].

The two-sequential ET reactions between Q_A and Q_B have been subjected to extensive kinetic optical studies [2–4]. Notably, it has been reported that the first ET from Q_A to Q_B is at least biphasic [5–8] with a fast phase (5–10 μs) that is assigned to pure ET and a slow phase (100–200 μs) which appears kinetically gated by a conformational change [9]: following light absorption, the slow phase of ET to Q_B first involves a conformational change followed by an ET step. Several possible structural changes involved in the gating process have been proposed. In addition to the structural changes, proton uptake also plays an important role in the electron transfer. Although the first ET to Q_B in isolated RCs does not involve the direct protonation of the semiquinone itself, substoichiometric proton uptake by the protein following formation of Q_B^- has been experimentally measured [10–13] and also predicted from electrostatic calculations [14–27], based on the X-ray structures. Proton binding by the RC protein reveals a change of the pK_a of amino acid side chains between the states Q_B and Q_B^-.

High resolution structures of the RCs from two purple bacteria, *Rb. sphaeroides* [28–32] and *Blastochloris (B.) viridis* [33–35] show that, unlike Q_A, Q_B is surrounded by many polar and acid residues of the L, M, and H protein subunits. In the *Rb. sphaeroides* RC, the Q_B binding pocket is formed by a cluster of polar and acid residues (and water molecules) including Ser-L223, Asp-L213, Asp-L210, Asp-M17, Glu-H173, and Glu-L212 [36,37]. In particular, Ser-L223, Asp-L213, and Glu-L212, which are all located near Q_B (Fig. 2), were shown to be crucial for rapid coupled electron-proton transfer to reduced Q_B [2–4]. Several other amino acid side chains located between the Q_B site and the surface [2–4] are also potential proton transfer species (such as Asp-L210, Asp-M17, Glu-H173, and Arg-L217). One controversial issue is the binding position of Q_B. While the binding site of Q_A is well-defined, different locations of Q_B have been observed in the various crystallographic structures reported for both *Rb. sphaeroides* and *B. viridis* RCs, and two distinct main binding sites for Q_B have been discussed [30,35,36,38], i.e., a position proximal to the non-heme iron (closest to Q_A) with hydrogen bonds at both carbonyls, and a position termed the distal site displaced by ~4.5 Å (further from the non-heme iron) with only one carbonyl hydrogen bonded to the protein (Fig. 1B). On the other hand, there is a consensus on the location of Q_B^-, which places the semiquinone at the

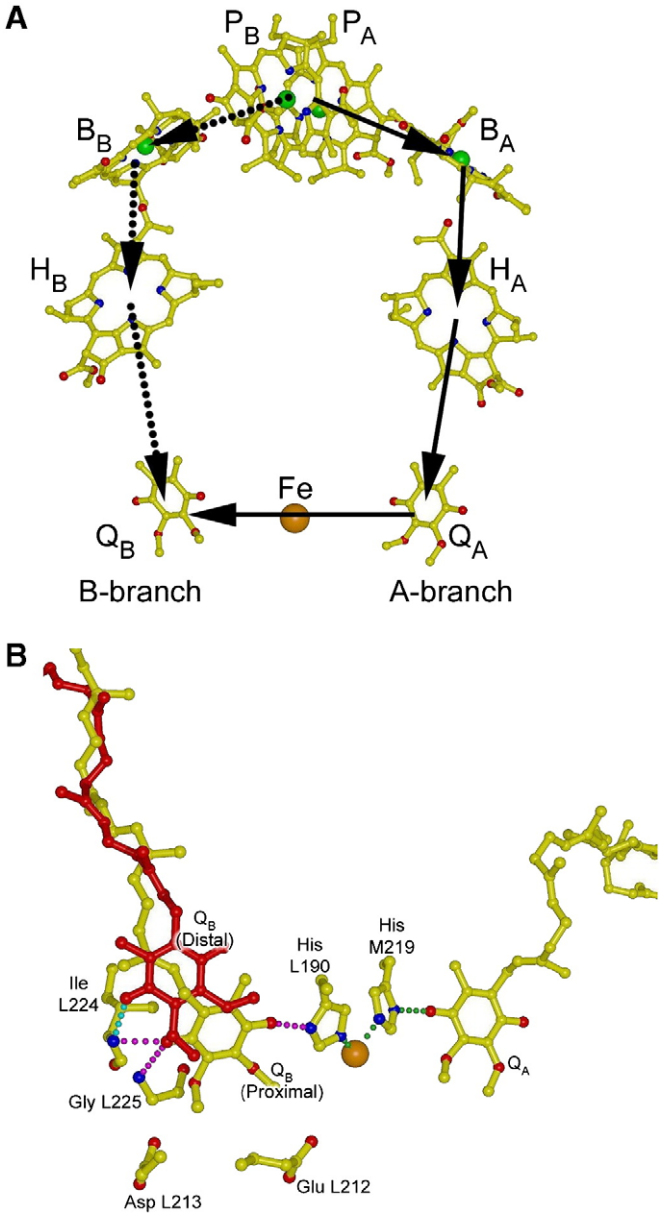

Fig. 1. Structural models of the *Rb. sphaeroides* reaction center. (A) Overall organization of the cofactors showing the bacteriochlorophylls (dimeric primary electron donor P and monomeric (B), bacteriopheophytins (H), and ubiquinones (Q). The cofactors are arranged around the axis of 2-fold symmetry in two branches (A and B) that span the membrane. The route of electron transfer from P to Q_B along the A-branch is shown by the solid arrows. (B) The distal and proximal binding positions of the Q_B ubiquinone in the RC. When in the distal position (red), the C4=O carbonyl accepts a hydrogen bond (green spheres) from the backbone NH group of Ile-L224, while the C_1=O carbonyl is free. When in the proximal position (green yellow), the C_1=O carbonyl is hydrogen-bonded (magenta spheres) to the backbone NH group of Ile-L224 and Gly-L225, while the C4=O carbonyl is hydrogen bonded to the side chain of His-L190. On the symmetrical side, His-M219 is a ligand to Q_A. This figure is courtesy of P. Fyfe and M.R. Jones (University of Bristol, Bristol, U.K.).

location proximal to the non-heme iron and at the approximate symmetry-related position of Q_A. In the proximal position, Q_B and/or Q_B^- form several likely hydrogen bonds to the backbone at L224 and/or L225 at the C_1=O carbonyl and to His-L190 at the C_4=O group [28,36]. Possible hydrogen-bonding interactions between Ser-L223 and Q_B and/or Q_B^- have been discussed [27,34–36,39–41] (see Section 2.4).

With respect to the general stucture-function relationship of Q_B and Q_B^-, the most specific questions that have been addressed and are still

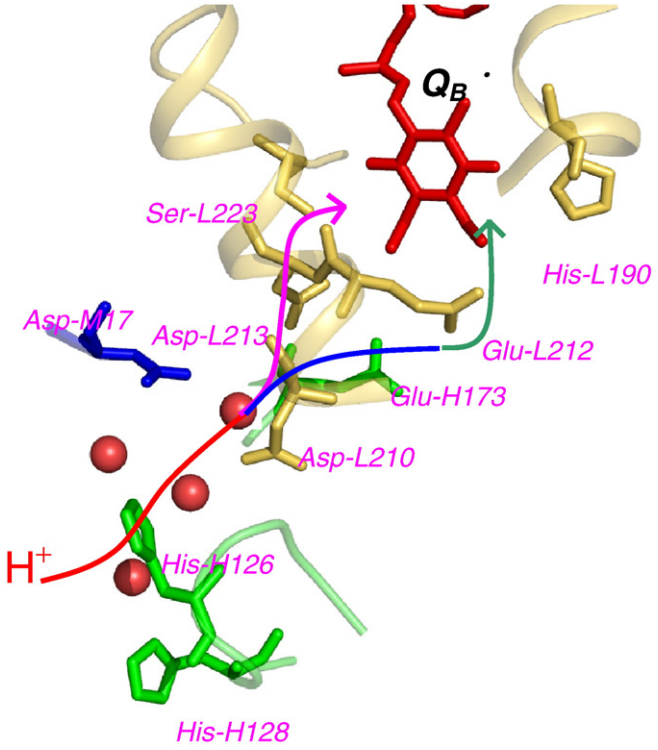

Fig. 2. Structure of the *Rb. sphaeroides* reaction center near the secondary quinone Q_B (from PDB ID code 1AIG, [36]). The arrows represent the general proton flow from the surface near His-H126 and His-H128 to reduced Q_B *via* Asp-L213 and Glu-L212. Located between the proton entry point and Glu-L212 are Asp-L210 and Asp-M17. In this work, we focus on mutations at Asp-L213, Glu-L212, Ser-L223, Asp-L210, Asp-M17, and Glu-H173. The red spheres represent bound water molecules. This figure is courtesy of M.L. Paddock (University of California, San Diego).

under debate are: 1) what are the pathways for proton transfer associated with Q_B reduction? 2) which amino acids are involved in proton uptake in response to the negative charge in their vicinity? 3) what is the gating step that governs the rate of the first ET from Q_A^- to Q_B? The first point has been extensively investigated by kinetic ET studies of native RCs and site-directed mutants in combination with the resolution of X-ray structures and several excellent reviews have appeared [2–4]. The second point has been extensively debated and is still controversial, there is no clear consensus between experimental (in particular FTIR) and theoretical work on the protonation states of key residues near Q_B and the extent of proton uptake by these residues upon Q_B^- formation. The third point has not yet been resolved and several studies have suggested that protein structural changes, Q_B movement, charge relaxation and/or protonation events may play an important role in the gating process required before ET to Q_B. In this review, we will show that FTIR difference spectroscopy of Q_B reduction has successfully contributed to the understanding of the two latter points.

Analyzing proton binding sites with IR difference spectroscopy is especially suited because protonation/deprotonation reactions result in changes of molecular vibrational frequencies in the 1770–1700 cm^{-1} spectral domain where the C=O stretching mode from the COOH side chain group of protonated carboxylic acid residues (Asp and Glu) is the main contributor [42,43]. In 1995, an essential finding was that upon reduction of Q_B in *Rb. sphaeroides* RCs, one signal centered at 1728 cm^{-1} in light-induced FTIR difference spectra [44] and a kinetic signal measured at 1725 cm^{-1} [45] which were sensitive to $^1H/^2H$ isotopic exchange were identified as the signature of proton uptake by a carboxylic acid group, suggesting that this amino acid was partially ionized at pH 7 in the Q_B neutral state and becomes protonated in the Q_B^- state. The 1728–1725 cm^{-1} signal was missing in the Glu-L212 to Gln mutant RC [44–46] and futher FTIR studies have demonstrated that it was indeed present in mutant RCs at a number of the other carboxylic acid sites in the vicinity of Q_B [44,46–48]. This signal was assigned to substoichiometric proton uptake by Glu-L212 upon Q_B^- formation. It was concluded that Glu-L212 in *Rb. sphaeroides* [44–48] and *Rb. capsulatus* [49,50] RCs is at least partially ionized at pH 7 in the neutral Q_B state becoming more protonated in the Q_B^- state. In addition, no spectral IR changes from Asp-L213 could be identified in the Q_B^-/Q_B FTIR spectra of *Rb. sphaeroides* RCs, and thus it was inferred that Asp-L213 does not significantly change protonation state upon Q_B^- formation in native RCs at pH 7 and is mostly ionized in both the Q_B and Q_B^- states [44].These IR conclusions were in disagreement with the interpretation of several experimental results based on the pH dependence of the first ET rate constant, the $P^+Q_B^-$ charge recombination kinetics, and the proton uptake stoichiometry by the Q_B^- state in native and mutant RCs from *Rb. sphaeroides* and *Rb. capsulatus* [10–12,51–58]. In general, these spectroscopic studies indicated that Glu-L212 contributes to proton uptake only at high pH and is essentially protonated at pH 7. Although early electrostatic calculations of proton uptake associated with Q_B reduction in *Rb. sphaeroides* indicated that the proton uptake was dominated by Glu-L212 [14,15], most of the subsequent calculations [19,21–23,26,27] were in contrast to the IR results. Thus, there was no consensus between experimental (FTIR) and theoretical work on the protonation states of the two key residues, Glu-L212 and Asp-L213 in the Q_B neutral state and on the extent of proton uptake by these residues upon Q_B^- formation. However, most of the electrostatic calculations predicted that a cluster of acids composed of Asp-L210, Asp-L213, and Glu-L212, exhibiting non-classic titration behavior, shares one proton in the Q_B state and two protons in the Q_B^- state, although the exact location of the protons varied amongst the studies. In particular the protonation states of Glu-L212 and Asp-L213 for a given Q_B or Q_B^- state can vary from no protonation to full protonation, depending on the molecular dynamics simulation technique and the X-ray structural RC model used [21,27]. Also, for both *Rb. sphaeroides* and *B. viridis* RCs several mechanistic models of the Q_B turnover have been discussed on the basis of X-ray structures [35,59,60] and electrogenic events [61–63]. Very recently, a model involving a cluster of strongly interacting carboxylic acids near Q_B led to revisit the interpretation of the highest pH band in measurements of proton uptake by the Q_B^- state in *Rb. sphaeroides* RCs [64].

In this review, we will first examine the approach of FTIR difference spectroscopy to investigate whether Q_B moves upon reduction in relation with the different locations of Q_B observed in the various crystallographic structures of the RC and the proposal that the movement of Q_B from its distal to proximal site accounted for the conformational gate limiting the rate of the first ET from $Q_A^-Q_B$ to $Q_AQ_B^-$. The binding site of Q_B has been explored using isotope-edited FTIR spectroscopy, a method that provides highly specific vibrational "fingerprints" of the bonding interactions of Q_B with the protein [40,65–71]. In the second section, we will review the contribution of the various experimental measurements, theoretical calculations, and molecular dynamics simulations which have been actively conducted to propose which amino acid side chains near Q_B could be proton donors/acceptors. In the two subsequent sections, we will show how FTIR spectroscopy of mutant RCs has directly allowed several carboxylic acids involved in proton uptake upon first ET to Q_B to be identified and how the observation of IR continuum bands led us to propose a direct role of bound water molecules in this reaction.

2. Interactions of Q_B and Q_B^- with the RC protein

2.1. Vibrational FTIR spectroscopy favors a unique Q_B binding site at the proximal position

2.1.1. The two main binding sites for Q_B in RC crystals

In crystals of native RCs from *Rb. sphaeroides*, the description of two main binding sites for Q_B (Fig. 1B) has provided a molecular basis

for a conformational gating model limiting the rate of the first ET from Q_A^- to Q_B [7,9]. A major finding was reported by Stowell et al., [36] when these authors obtained, at cryogenic temperature, the dark-adapted and light-adapted structures (at 2.2 and 2.6 Å resolution, respectively) for RCs containing a mixture of native Q_B and added ubiquinone-2. In the dark-adapted state (PQ_B), Q_B was mainly found in the distal position with only one carbonyl (C_4=O) of Q_B interacting with the backbone (Ile-L224). In the charge-separated state ($P^+Q_B^-$) of RCs, Q_B^- was located ~4.5 Å from the Q_B distal position in the neutral PQ_B state and had undergone a 180° ring flip: Q_B^- occupies a proximal position with both carbonyls hydrogen bonded to the protein (Fig. 1B). These results were later confirmed by Fritzsch et al., [38], although in the dark neutral state (at 1.87 Å resolution) the occupancies were 55% and 45% for the distal and proximal sites, respectively, whereas in the light-excited state (at 2.07 Å resolution), the occupancies were 10% and 90%, respectively. In *B. viridis* RCs, a mechanistic model involving a similar displacement of Q_B from the distal to the proximal site has also been proposed by Lancaster and Michel [35,59,60].

The motion of Q_B from the distal to the proximal site was proposed to represent the conformational gate that limits the rate of the first ET from $Q_A^-Q_B$ to $Q_AQ_B^-$ [9,36]. The proximal site was postulated to be an activated site for ET, whereas the distal site was assumed to be inactive in ET. This mechanism would account for the observation that RCs cooled under illumination are frozen in an active state (i.e., in the $P^+Q_B^-$ charge-separated state) but RCs trapped at low temperatures in the dark (i.e., in the PQ_B state) are inactive for the $Q_A^-Q_B$ to $Q_AQ_B^-$ ET [7,72,73]. This has been called the "Kleinfeld effect" [72] which has also been observed recently in *B. viridis* RCs with EPR and ENDOR techniques [74].

The conformational gating mechanism has triggered a number of theoretical works on the functional implications of the two distinct binding sites of Q_B. Calculations on the energetics of the ET from Q_A^- to Q_B in *Rb. sphaeroides* RCs have indicated that ET is more favorable when Q_B is in the proximal site [21]. Molecular dynamics simulations of Q_B binding in the RC of *Rb. sphaeroides* [22] and *B. viridis* [35,59,60] support the spontaneous transfer of Q_B from the distal site to the proximal site, notably when the primary quinone becomes reduced. The existence of two binding sites has been proposed to be related to different protonation states of the two nearby amino acids Glu-L212 and Asp-L213 [22,23] that are important for rapid electron-coupled proton transfer to reduced Q_B. A mechanistic model of the Q_B turnover in *Rb. sphaeroides* RCs also assumed two possible configurations of the quinone depending on the equilibrium between the ionized and protonated forms of Glu-L212 [62,63]. The orientation of the Glu-L212 side chain was described as the possible conformational gate for the Q_B migration which may control the first ET [23]. More recently, it has been also proposed that the Ser-L223 hydroxyl proton flip between Asp-L213 and Q_B upon its reduction could contribute to the gating step [27,39,41]. Importantly, pH [26], ubiquinone isoprene chain length [35], temperature, and cryoprotectant [75] have been reported to likely influence the binding position of Q_B.

2.1.2. Isotope-edited FTIR spectra of Q_B in native Rb. sphaeroides and B. viridis RCs

Besides X-ray crystallography, the binding of quinones (Q_A and Q_B) can be investigated by isotope-edited FTIR spectroscopy which provides a way to determine the bonding interactions of Q_B (Q_A) and Q_B^- (Q_A^-) with the protein in RCs [67]. FTIR difference spectroscopy is an extremely sensitive method for investigating atomic interactions at the level of individual bonds. In the case of a large molecular system such as the RC, the complexity of IR spectra can be overcome by using a difference technique whereby the FTIR spectrum of the ground state of the protein is subtracted from that of a well-defined charge-separated state. Using such a difference procedure, only the groups that alter their molecular vibrations between these two states will contribute to the difference spectrum, whereas all the vibrational modes from groups that do not participate to the reaction will cancel out [42,43,76–78]. By combining this technique with isotope labeling, it is possible to detect and assign vibrational modes of single chemical groups in a protein complex as large as a RC [67,79]. Furthermore, the IR frequency of carbonyl bonds is strongly influenced by the surrounding environment (electrostatics and polar interactions) [80].

Precise IR fingerprints of the interactions of Q_B before and after photoreduction have been obtained for wild-type RCs from *Rb. sphaeroides* and *B. viridis* RCs [65–67,70] as well as for a series of mutant RCs [40,68,69,71], using RCs reconstituted with ubiquinone-3 site-specific ^{13}C-labeled either at the C_1=O or C_4=O carbonyl. The molecular vibrations of Q_B and Q_B^- can be specifically revealed by calculating double-difference spectra between the Q_B^-/Q_B spectra recorded with ^{13}C-labeled and unlabeled ubiquinone. For both *Rb. sphaeroides* (Fig. 3a and e) and *B. viridis* [65] RCs, the IR fingerprint spectra for $^{13}C_1$ and $^{13}C_4$ labels show a unique C=O band for neutral Q_B at 1641 cm^{-1} that is downshifted by 10–20 cm^{-1} compared to the frequency of the free carbonyls of the quinone in solution [81]. These IR data are indicative of symmetrical hydrogen bonding of Q_B to the binding site with moderate hydrogen-bonding strength [65,66]. Thus, the two carbonyls of Q_B interact with the protein, as it is described in the various X-ray structures of native and mutant RCs when Q_B occupies the proximal site (Fig. 1B). Moreover, the IR fingerprint of the semiquinone Q_B^- shows a main negative band at 1479 cm^{-1} (Fig. 3a and e) which is similarly shifted to 1439 cm^{-1} (positive peak in Fig. 3a and e) by either $^{13}C_1$ or $^{13}C_4$ labels, thus also favoring symmetrical

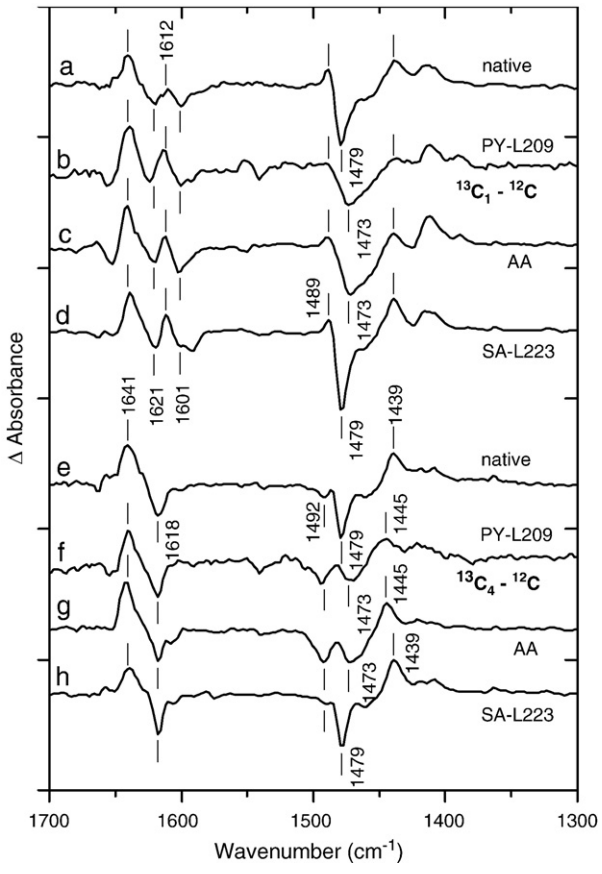

Fig. 3. Comparison of isotope-edited Q_B^-/Q_B FTIR fingerprint spectra (isotopically labeled minus unlabeled) obtained for wild type and mutant RCs from *Rb. sphaeroides* reconstituted with $^{13}C_1$-labeled ubiquinone Q_3 (a–d), and $^{13}C_4$-labeled Q_3 (e–h). (a,e) native RCs, pH 8, (b,f) Pro-L209→Tyr (PY-L209), pH 7, (c,g) Asp-L213→Ala/Glu-L212→Ala (AA), pH 8, (d,h) Ser-L223→Ala (SA-L223), pH 7. Each division on the vertical scale corresponds to 10^{-4} absorbance unit and the frequency of the peaks is given at ±1 cm^{-1}. These conditions apply to all subsequent figures.

interactions of the two carbonyls of Q_B^- with the protein in *Rb. sphaeroides* RCs [65]. In contrast, the IR fingerprint spectra of the quinone Q_A in *Rb. sphaeroides* show a large difference in the frequency of the two C=O modes at 1660 and 1601 cm^{-1}, indicative of a pronounced asymmetry in hydrogen bonding, with a very strong hydrogen bond between the C_4=O carbonyl at 1601 cm^{-1} and His-M219 [82–84].

2.1.3. Isotope-edited FTIR spectra of Q_B in Rb. sphaeroides mutant RCs

The recent observation that Q_B was found to bind essentially in the proximal position in the crystallographic structures of several mutant RCs from *Rb. sphaeroides*[85–87] near the Q_B site offered an attractive opportunity to test the IR proposal that functional Q_B in both native *Rb. sphaeroides* and *B. viridis* RCs occupies the site corresponding to the proximal position and to discuss the implications of these new results for the conformational gate of the first ET from to Q_A^- to Q_B.

Mutations at Pro-L209 were originally constructed to interrupt a water chain in the RC protein [30,88]. Interestingly, in the dark-adapted crystals of Pro-L209→Tyr RCs at 5 °C, only one site is described for the location of Q_B which is the proximal one [86]. Moreover, the first ET to Q_B in this mutant is not significantly changed relative to that of native RCs [89,90], which is not expected if the movement of Q_B represents the dominant contribution to the rate-limiting step controlling the first ET to Q_B. In crystals of the Pro-L209→Phe mutant RCs, the best fit for Q_B was obtained for an intermediate position of Q_B between the distal and proximal binding sites [86]. The isotope-edited double-difference spectra of the Tyr-L209 mutant RC [68] are shown in Fig. 3b and f. For the neutral Q_B, these spectra together with those of the Phe-L209 mutant RC [71] were essentially the same as those for wild type RCs (Fig. 3a and e), i.e., showing a unique C=O band at 1641 cm^{-1}, and thus demonstrating an identical bonding pattern of the neutral ubiquinone to the protein in these two mutant RCs at L209 [68,71]. In contrast, large perturbations of the semiquinone modes (1500–1400 cm^{-1} spectral range) were observed in the Q_B^-/Q_B spectra of the PF-L209 and PY-L209 mutant RCs, notably at 1489 and 1473 cm^{-1} upon $^{13}C_1$ labeling (Fig. 3b) and at 1492 and 1473 cm^{-1} upon $^{13}C_4$ labeling (Fig. 3f).

The first mutant RC from *Rb. sphaeroides* that has provided clear evidence from X-ray studies for Q_B being bound in the proximal site with high occupancy contains the mutation Ala-M260 to Trp, resulting in the absence of Q_A in the RC and thus the A-branch ET to Q_A (Fig. 1A), and a fortiori to Q_B was abolished [85,91]. However, B-branch (Fig. 1A) active mutant RCs with additional mutation(s) to the one at Ala-M260 have been subsequently constructed (e.g., the double mutant Ala-M260→Trp/Leu-M214→His and the quadruple mutant, denoted WAAH, containing the additional mutations Glu-L212→Ala and Asp-L213→Ala) and characterized by spectroscopic techniques [92], including FTIR spectroscopy of the Q_B reduction [69,93]. Although the high resolution structures of the double and quadruple mutants quoted above have not yet been resolved, X-ray diffraction studies of the double Glu-L212→Ala/Asp-L213→Ala (denoted AA, see Table 1) mutant RC [87] show that Q_B is bound mostly in the proximal site, as seen previously in the structures of the Ala-M260→Trp [85] and Pro-L209→Tyr [86] mutant RCs. Note that in the AA RC, reduction of Q_B beyond the semiquinone state is prevented [94]. Isotope-edited double-difference spectra have been obtained for the AA (A-branch active RC) and WAAH (B-branch active RC) mutants. The IR fingerprints for the C=O and C=C modes of Q_B in the AA (Fig. 3c and g) and WAAH mutants [69] were essentially the same as those previously reported for native RCs (Fig. 3a and e), thus demonstrating identical bonding interactions between Q_B and the protein in all these RCs. These IR results also demonstrate that Q_B occupies the same binding position proximal to the non-heme iron prior to reduction by either A- or B-branch ET [69].

The position of neutral Q_B in the crystals of the above described mutants [85–87] was thus found to be similar to the one found for native RCs after light-adaptation at low temperature [36,38]. When Q_B was found in the proximal site in dark-adapted crystals of native or mutant RCs, the secondary quinone was presumed to be in the neutral state since no special illumination of the crystals was performed. However, the possibility that Q_B is reduced in the crystal during the collection of X-ray data, at least at room temperature, has been questionned [36,85,95,96]. On the other hand, when the quinone is found in the distal site [30,36,87,97] it is not excluded that the ubiquinone is present as quinol [30]. Therefore, the redox state of the quinone observed in the distal and proximal sites of RC crystals still presents some ambiguity. Another example is found in frozen crystals of the Asp-L213→Asn mutant RC where the position of the quinone was found to be proximal but Q_B^- is likely to be the prevalent state due to its enhanced stability over the neutral state in this mutant [98].

Table 1
Nomenclature of mutant reaction centers

Amino acid							
Name	L212	L213	L210	M17	H173	L209	L223
Wild type	Glu	Asp	Asp	Asp	Glu	Pro	Ser
SA-L223							Ala
EQ-L212	Gln						
ED-L212	Asp						
DN-L213	Asn						
DE-L213		Glu					
EA-L212/DA-L213 (AA)	Ala	Ala					
ED-L212/DE-L213	Asp	Glu					
ED-L212/DQ-L213	Asp	Gln					
EN-L212/DE-L213	Asn	Glu					
DN-L210			Asn				
DN-M17				Asn			
EQ-H173					Gln		
PY-L209						Tyr	
PF-L209						Phe	

With FTIR spectroscopy, it should be emphasized that a control of the functionality of the quinone at the Q_B site can be performed in the conditions of the FTIR experiments by measuring the characteristic oscillation pattern with a period of two when the quinone evolves between the states Q_B, Q_B^-, and Q_BH_2 upon excitation of RCs with a sequence of flashes [99,100]. Notably, it has been demonstrated that upon sequential flash excitation of RCs, the shape of the light-induced FTIR difference spectra exhibits a clear fingerprint for Q_B^- formation on odd-numbered flashes and distinct features on even-numbered flashes [101,102]. Although the one-electron reduction of the secondary quinone has been monitored in RC crystals [36,103], the oscillatory behavior of the formation and destruction of the semiquinone state on a sequence of successive flashes has not been reported so far for the secondary quinone in RCs crystals. Another advantage of using FTIR spectroscopy is that IR samples do not contain additives such as the crystallizing agents needed to generate crystals or cryoprotectants when freezing the sample for optical studies [90].

To summarize the FTIR data on mutant RCs, the same isotope-edited IR fingerprints for the two carbonyls of neutral Q_B have been observed for native *Rb. sphaeroides* RCs and mutant RCs at the Pro-L209 [68,71], Ala-M260 [69], and Glu-L212/Asp-L213 [69] sites for which X-ray crystallography has found the quinone in the proximal position. In contrast, large perturbations of the semiquinone modes have been observed in the Q_B^-/Q_B spectra of all these mutant RCs (Fig. 3b, c, f and g). The symmetrical hydrogen-bonding pattern indicated by the unique 1641 cm^{-1} C=O band for the unlabeled neutral Q_B in native and mutant RCs fits the description of the proximal site, with both carbonyls of Q_B engaged in equivalent hydrogen-bond interactions with the surrounding protein. Therefore, there is a good correlation between the results of FTIR spectroscopy and X-ray crystallography for these mutant RCs. Consequently, our

FTIR data strongly favor the proximal position for neutral Q_B in native functional RCs from *Rb. sphaeroides* and *B. vridis* in contrast with the distal Q_B structure found in dark-adapted crystals of native *Rb. sphaeroides* RCs [30,87,97,98]. Moreover, our FTIR results on *B. viridis* RCs are in full agreement with the earlier refinement of a dark structure showing ubiquinone-2 to occupy only the proximal site [35] and time-resolved crystallographic studies of *B. viridis* RC crystals at room temperature [104] showing a single proximal binding site for the quinone for both the light-and dark-adapted states. A more recent structure of the *B. viridis* RC at 2.2 Å resolution has been determined at 100 K on flash-freezed crystals and it also supports predominant binding of Q_B in the proximal position in both the neutral and charge-separated states [96]. As emphasized by Baxter et al., [96,104] these X-ray data do not support a large-scale motion of the quinone between the Q_B and Q_B^- states in *B. viridis*.

2.2. Vibrational FTIR spectroscopy of Rb. sphaeroides RCs shows that Q_B does not move upon reduction

Isotope-edited FTIR difference spectroscopy was further used to compare in native *Rb. sphaeroides* RCs the hydrogen-bonding states of Q_B and Q_B^- at room temperature, where Q_B is free to move upon photoreduction, and at 85 K, where such a motion cannot occur [70]. If it is assumed that the displacement of Q_B between the distal and proximal position takes place as proposed in the conformational gating mechanism of Stowell et al., [9,35,36,59], then $P^+Q_B^-/PQ_B$ FTIR difference spectra measured at 290 K will probe the bonding interactions of neutral Q_B located in the distal site and of Q_B^- in the proximal site. Cooling RCs under illumination should lead to the trapping of Q_B^- in the proximal position. When left at 85 K in the dark, a large fraction of the $P^+Q_B^-$ state will return to the PQ_B ground state without any possibility of movement of the quinone to the distal position, due to the cryogenic temperature. Specific experimental conditions are described in [70]. The IR frequency of the two carbonyls of neutral Q_B should, therefore, be noticeably different in measurements performed at the two temperatures. However, a unique C=O frequency at 1641 cm^{-1} was found for the two carbonyls of Q_B at both 85 K and 290 K [70]. Moreover, the similarity of the isotope-edited IR fingerprints for the interactions of Q_B and Q_B^- with the protein measured at 85 K and 290 K makes it unlikely that the quinone moves appreciably upon photoreduction at room temperature[1]. It is therefore concluded that at room temperature both Q_B and Q_B^- occupy a single and unique binding site that fits well the description of the proximal site derived from X-ray crystallography. The role of the distal site however remains not clear [105].

2.3. Possible alternative gating mechanisms of the first electron transfer to Q_B

Although the distal to proximal change of position of the quinone has been given important functional relevance for the gating process of the Q_A^- to Q_B ET, it should be recognized that recently, several approaches other than FTIR [68–71] have also emphasized that the movement of Q_B is unlikely to be the dominant contribution to the conformational gate that controls the first ET to Q_B in native RCs. Notably, the slow phase of the ET rate from Q_A^- to Q_B in *Rb. sphaeroides* RCs has been found to be independent of the isoprene chain length of Q_B [7,90,106,107], which is unexpected if Q_B needs to undergo rotation and displacement in the rate-limiting step. In agreement with these experiments, FTIR studies of wild type RCs from *Rb. sphaeroides* have shown that the IR fingerprint of Q_B does not change upon varying the isoprene chain length from 1 to 10 isoprene units [65,66]. These FTIR results therefore do not indicate an influence of the tail length on the interactions of Q_B with the protein, and thus on its position within the RC. Moreover, the absence of a significant change in the first ET rate in the Pro-L209→Tyr mutant (where Q_B occupies the proximal position) relative to native RCs is not consistent with the movement of Q_B representing the rate-limiting step [89,90].

Alternative sources of protein conformational change, proton and/or water molecule movements (water exclusion), charge relaxation, protonation events, [6,106] might contribute to the gating mechanism, such as the observed protonation of Glu-L212 coupled with ET from Q_A^- to Q_B [44,45,48]. However, the slow phase of the first ET rate in the Glu-L212→Gln mutant RCs at pH < 8.5 is the same as in native RCs [51,53,108], which does not favor the protonation of Glu-L212 to be involved in the gating mechanism. Recent electrostatic calculations have suggested that the orientation of the hydroxyl Ser-L223 (Fig. 2) which could alternatively form a hydrogen bond to either Asp-L213 or Q_B/Q_B^- could play a role in conformational gating for the first ET reaction [27,39]. It has been proposed that the orientation of the Ser-OH group changes upon Q_B reduction and when Q_B is reduced, Ser-L223 becomes a hydrogen-bond donor to the anionic semiquinone [41]. The rotation of the Ser OH proton from Asp-L213 to Q_B^- is expected to be an important step in the proton transfer to the reduced quinone. To investigate possible hydrogen-bonding interactions between Ser-L223 and Q_B and/or Q_B^-, we thus applied the technique of isotope-edited FTIR difference spectroscopy to the Ser-L223→Ala mutant RC [40], as described in the next section.

2.4. Vibrational FTIR spectroscopy shows that Ser-L223 is not a ligand of Q_B or Q_B^-

In the RC from *Rb. sphaeroides*, when the quinone lies in the proximal site, the hydroxyl side chain of Ser-L223 is in the vicinity (~3 Å) of the C_1 carbonyl of Q_B/Q_B^- (Fig. 2) and therefore may form a hydrogen bond [34,36] which has been experimentally proposed from ENDOR spectroscopy of Q_B^- at 77 K [41]. Early studies have shown that mutation of Ser-L223 inhibits the turnover of Q_B [109,110] as well as the binding of competitive inhibitors [111,112]. The functional importance of Ser-L223 can be explained by fast proton transfer through a transiently-formed hydrogen bond between Ser-L223 and Q_B^-. This model would explain the decreased rate of proton-coupled electron transfer in RCs with Ser-L223 replaced with Ala in *Rb. sphaeroides* and *B. viridis* [109,110,112,113].

On the other hand, electrostatic calculations [27,39] have shown that the Ser hydroxyl orientation depends on the charge of Asp-L213. If Asp-L213 is ionized when Q_B is neutral, the side chain of Ser-L223 is found to point towards the Asp side chain, away from Q_B. When Asp-L213 is protonated, Ser-L223 donates a proton to Q_B with 80% probability. In both cases, Ser-L223 is a hydrogen-bond donor to the semiquinone Q_B^-. In addition, molecular dynamics simulations of the Q_A^- to Q_B ET indicate a faster time constant for the reaction when a hydrogen bond is present between Ser-L223 and Q_B^- [39]. However, comparable simulations for the Ser-L223→Ala mutant RC emphasize that a hydrogen bond is not necessary for the ET process from Q_A^- to Q_B to occur but may play a crucial role in the reaction kinetics [39].

Upon removing the potential hydrogen bond, perturbations of the carbonyl vibration frequencies of Q_B/Q_B^- should reflect the magnitude

[1] After completion of this review, we became aware of the conclusion derived from the EPR work of Heinen et al., [174] on the charge-separated state $P^+Q_A^-$ that upon reduction of Q_A, the quinone ring rotates by 60° within its plane. The authors propose that this large rotation indeed represents the conformational change that gates the Q_A^- to Q_B ET step. This conclusion is totally incompatible with the result of a previous study dealing with the investigation of a possible motion of Q_A upon photoreduction using isotope-edited FTIR difference spectroscopy [82]. In this study, it was demonstrated that the frequency of the C_1=O and C_4=O carbonyls of Q_A and of Q_A^- were essentially the same when the photoreduction was performed either at 5 °C, when the quinone could move, or at 100 K, when such motion cannot occur. The frequency of the two carbonyl vibrations which reflects their specific bonding interactions with the RC protein in the state Q_A (highly asymmetrical interactions) and Q_A^- (less asymmetrical), provides a set of highly sensitive fingerprints for these interactions. Therefore we had previously concluded that Q_A does not move appreciably upon reduction [82].

of the hydrogen-bonding interactions. The Ser-L223→Ala mutant RC (Table 1) was reconstituted with site-specific ^{13}C-labeled ubiquinone. The isotope-edited IR fingerprint spectra for the C═O and C═C modes of Q_B and the C···O and C···C modes of the semiquinone in the mutant (Fig. 3d and h) are essentially the same as those of the native RC (Fig. 3a and e). These findings indicate that highly equivalent interactions of Q_B and Q_B^- with the protein occur in both native and mutant RCs. The FTIR study of the SA-L223 mutant thus demonstrates that the removal of the hydroxyl side chain in the SA-L223 mutant has essentially no effect on the quinone and semiquinone modes of Q_B [40]. Assuming that in native RCs the C_1 carbonyl of the quinone interacts with the hydroxyl of Ser-L223 in the Q_B and/or Q_B^- states, as proposed from some X-ray data [28,29,31,36], electrostatic calculations [19,27,39] as well as from recent ENDOR experiments at 77 K [41], we would have expected to observe changes in the IR fingerprint pattern of the quinone/semiquinone modes of the Ser-L223→Ala mutant RC. A possible explanation for the apparent discrepancy between FTIR [40] and ENDOR [41] results would be that hydrogen bonding between Ser-L223 and Q_B or Q_B^- might be temperature dependent.

The FTIR results therefore demonstrate that Ser-L223 does not have a significant interaction with either Q_B or Q_B^- in the native RC at 15 °C. The simplest model to explain the FTIR data is that the Ser-L223 hydroxyl group forms a more stable hydrogen bond with another group than with the C_1 carbonyl group of the quinone. The most likely candidate would be Asp-L213, which is located within hydrogen-bonding proximity (see e.g. [36]) and has been calculated to form a stable hydrogen bond when Asp-L213 is ionized [19,27,39]. These results imply that Asp-L213 retains some ionized character in the Q_B^- state as it has been previously proposed from FTIR results which do not show changes of protonated carboxylic bands associated with Asp-L213 upon Q_B^- formation [44,114] (see Section 4.4). The FTIR model cannot exclude that a small fraction (<5%) of the Ser OH groups may be hydrogen bonded to Q_B^- [40]. However, if a hydrogen bond is transiently formed in the proton transfer to the reduced quinone, it cannot be a major factor in determining the energy of the conformational gate associated with the first ET to Q_B [9] since the observed first ET rates in the native and the SA-L223 RCs remains similar [109,110]. Other interactions of larger magnitude are likely involved in the conformational gate. Paddock et al., [105] have recently proposed that the large difference in the lifetimes of the unrelaxed and relaxed $P^+Q_B^-$ states demonstrates that energetically significant conformational changes are involved in stabilizing $P^+Q_B^-$ state, and they have suggested that the unrelaxed and relaxed states can be considered to be the initial and final states along the reaction coordinate for conformationally gated ET [105].

3. Experimental results and theoretical calculations of proton uptake in the bacterial RC upon Q_B reduction

3.1. Proton uptake stoichiometry by the Q_B^- state in Rb. sphaeroides and Rb. capsulatus RCs

The pH dependence of the proton uptake upon formation of Q_B^- (and Q_A^-) has been measured by using pH-sensitive dyes and/or glass pH electrodes for *Rb. sphaeroides* and *Rb. capsulatus* RCs [10,11] and electric conductimetry [115,116]. The titration curves (H^+/Q_B^-) for *Rb. sphaeroides* and *Rb. capsulatus* RCs show two distinct maxima at pH ~6 and ~10–11 that have been fitted to 4 or 5 protonable groups with distinct pK_as [11,12,56]. The group with the highest pK_a (pK_a ~9.5–10.5) has been for a long time associated with Glu-L212 [12,56] by comparison with data obtained from the pH dependence of kinetic ET rates in native and mutant RCs [51,53], as described below. Moreover, it has been further shown that the high pH maximum of the H^+/Q_B^- titration curve disappeared in the Glu-L212→Gln mutant [55,57], which has corroborated the suggested proposal.

The pK_a of Glu-L212 and Asp-L213 were first estimated from the pH dependence of kinetic ET rates which are sensitive to the charges near Q_B, i.e., to the ionization state of all charged species near Q_B, including Glu-L212 and Asp-L213. In native RCs, both the forward ET rate Q_A^- to Q_B (k_{AB}) and the recombination reaction rate $P^+Q_B^-$ to PQ_B (k_{BD}) are pH-dependent above pH ~9 and below pH ~7 [12,51–55,94]. These kinetic results indicate interaction of Q_B with amino acid side chains with a pK_a near 9.5 and 4–5, respectively. On the basis of the comparison of the pH dependence of the ET rates in native and mutant RCs, it was initially proposed by Paddock et al., [51] that in *Rb. sphaeroides*, Glu-L212 has an unusually high pK_a of 9.5. It has been observed that in the Glu-L212→Gln mutant k_{AB} and k_{BD} are essentially pH independent in the pH range from 7 to 11. The straightforward interpretation of these data was that the high pH variation of ET kinetics in the native RC is due to Glu-L212, which thus has an anomalously high pK_a value of 9.5+0.3. Such a high pK_a value for Glu-L212 was also suggested by Takahashi and Wraight [53]. In contrast, for mutant RCs at Asp-L213, k_{BD} was found to be essentially independent of pH below pH 6 and Asp-L213 was estimated to have an apparent pK_a of ~4–4.5 [52–54]. The protonation state of Asp-L213 was inferred from the much slower recombination rate k_{BD} observed in the Asp-L213→Asn mutant compared to that of native RCs and it was proposed that Asp-L213 is ionized in both Q_B and Q_B^- states [52–54].

Therefore, proton uptake measurements in native RCs and kinetic ET data on native and mutant RCs have supported the idea of the involvement of Glu-L212 as a carboxylic acid residue near Q_B having a pK_a near 9.5 in the Q_B state that is shifted to >10.5 in the Q_B^- state [10,12,53,55–57]. Thus, Glu-L212 would contribute to proton uptake essentially at high pH. Also, light-induced photovoltage changes upon formation of Q_B^- measured in native *Rb. sphaeroides* and the Gln-L212 mutant led to assign a pK_a value of about 9.5 to Glu-L212 [58]. On the other hand, FTIR data on *Rb. sphaeroides* [40,44–48] and *Rb. capsulatus* [49,50] show that Glu-L212 already contributes to proton uptake at pH 7 (and even at pH 4 for *Rb. sphaeroides*, see Section 5.1).

In 1994, the proton uptake upon Q_B^- formation was for the first time reported for the Glu-L212→Gln mutant and, surprisingly, at pH<7.5 it was essentially the same as in native RCs but at pH 8.5 it was smaller in the mutant than in the native RC [55]. These observations apparently confirm that Glu-L212 has a significant contribution to the proton uptake at pH >7.5, in agreement with the conclusions reached from the pH dependence of the charge recombination kinetics k_{BD}[51]. However, it was already emphasized [55] that because Glu-L212 interacts strongly with other residues (e.g., Asp-L213, Asp-L210), the effect on proton uptake due to replacements at the L212 position was difficult to predict. Furthermore, it was shown that when Glu-L212 and/or Asp-L213 were changed to the non protonable residues Gln and Asn, respectively, proton binding kinetics were severely impeded [52–54,108]. In particular, kinetic measurements of proton uptake at pH 8.5 after a single laser flash in native and Glu-L212→Gln mutant RCs show that the mutant displays greatly reduced amplitude of proton uptake (decreased 8 fold) [108]. It was thus suggested that the pK_a of Glu-L212 was around 8.5 [55,108,117].

In *Rb. capsulatus* RCs, the absence of pH dependence of k_{BD} in RCs of the double Ala mutant at L212 and L213 (AA in Table 1) apparently confirmed that Asp-L213 and Glu-L212 are responsible for the variations of k_{AB} in the pH range 4–7 and above pH 9.5, respectively, in the native RCs [94]. However, the recovery of RC function in a photocompetent suppressor mutant of the AA mutant which carried a third compensating mutation (Arg-M231 to Leu), i.e., the observation in this triple mutant of a pH dependency of k_{BD} that resembles that of native RCs, clearly indicates that the residue with a high pK_a cannot be Glu-L212 [94]. Thus, early in 1992, Hanson and coll., concluded that in *Rb. capsulatus* RCs, Glu-L212 and Asp-L213 are not obligatory residues in the pathways for proton donation to reduced Q_B and that in mutant RCs, protons can diffuse to reduced Q_B by alternative pathways. Those pathways could involve water molecules [94]. For both *Rb. sphaeroides* and *Rb. capsulatus* RCs, it was further reported that in RCs lacking Glu-L212 and/or Asp-L213, second-site mutations (for example the Asn-

M44→Asp substitution) can restore electron and proton transfer [13,57,118–120]. Also, the stoichiometry of the H^+/Q_B^- proton uptake in native RCs from *Rb. capsulatus*, in the mutant Glu-L212→Gln, and in a revertant of Gln-L212 with Arg-M231→Cys were measured to be essentially equivalent below pH 7.5 [57]. However, above pH 7.5–8, the single Glu-L212→Gln mutant and the revertant fail to take up protons, i.e., the high pH band was not present. These observations were thus again interpreted in terms of Glu-L212 being already protonated at neutral pH in native RCs [57]. Further studies of revertants in *Rb. capsulatus* [13] agreed with the hypothesis that Glu-L212 is essentially protonated at neutral pH. Therefore, all these observations were in striking contrast with the earlier proposal from FTIR and kinetic IR experiments that Glu-L212 at pH 7 is at least partially ionized in the Q_B state and becomes more protonated in the Q_B^- state [44,45].

A major change to this dogma, outside the conclusions from the FTIR studies, was brought by the study in *Rb. capsulatus* of a mutant at Ala-M247, the structural equivalent of Asp-L213 on the M-subunit of the RC. It was shown that the pH dependence of the H^+/Q_B^- proton uptake characteristic of native RCs was fully restored in the double Ala mutant at L212 and L213 (Table 1) when in addition Ala-M247 was replaced with a Tyr [13,121]. Moreover, the H^+/Q_B^- proton uptake was intensified in the Ala-M247→Tyr single mutant, as also observed in mutants at Pro-L209 [122]. The restoration of a native-like high pH band in the triple mutant (AA+ Tyr-M247) therefore indicates that the proton uptake detected at high pH is not specifically associated with Glu-L212. Moreover, a recent analysis of RC mutants at His-M266 (a ligand of the non-heme iron) also shows that the high pH peak observed in the native RC in the pH dependence of H^+/Q_B^- is no longer detected in the mutants with Leu or Ala at M266 [64]. Because of the putative strong interactions between several carboxylic acids close to Q_B, i.e., Glu-L212, Asp-L213, and Asp-L210, it was then suggested that the high pH band is not the signature of a particular group, but it reflects the response as a whole of such a strongly interacting acidic cluster to the formation of Q_B^- (and Q_A^-) [64,121,122]. Indeed, Cheap et al. [64] have recently modeled proton uptake by a cluster of four strongly interacting acid groups in response to semiquinone formation. The model shows that the deletion of any group results in the suppression of the high pH band [64]. On the basis of this strongly anticooperative model, the observation of the unspecific disappearance of the high pH band in all the mutants mentionned above as well as the restoration of this high pH band in revertants of the double Ala mutations at L212 and L213 could be explained [13,57,64,94,118,120,121].

3.2. Electrostatic calculations of proton uptake by carboxylic acids by the Q_B^- state in *Rb. sphaeroides* and *B. viridis* RCs

Electrostatic calculations have been conducted to explore the role of individual amino acids in modulating the free energy of the first ET from Q_A^- to Q_B and in determining proton uptake on the formation of Q_A^- or Q_B^-. The idea of a strongly interacting acidic cluster near Q_B has first emerged from electrostatic calculations [14–19] and X-ray structures [36,37]. A cluster of acids (Glu-L212, Asp-L313, and Asp-L210) and Ser-L223 near Q_B (Fig. 1B) was proposed to play important roles in the ET from Q_A^- to Q_B. According to the Henderson-Hasselbalch equation, an isolated acid group with a pK_a of 9.5 should be protonated at pH 7 and thus could not be further protonated upon Q_B^- formation. However, a cluster of acid residues near Q_B can have complex titration behavior due to electrostatic interactions within the cluster. Electrostatic calculations have been performed for RCs whose X-ray crystallographic structures have been resolved, i.e., for *Rb. sphaeroides* and *B. viridis*. Early calculations in *Rb. sphaeroides* [14,15] show that several titrating acid groups, including Glu-L212, Asp-L213, and Asp-L210, had a significant fractional ionization over a wide pH range (>5 pH units), contrary to the classical Henderson–Hasselbalch equation. The calculations of Gunner and Honig [14] and Beroza et al., [15] both predicted that the major contribution to proton uptake upon Q_B^- formation was the protonation of Glu-L212 due to the strong electrostatic coupling between the ionized Glu-L212 and Q_B^-, although differences in the detailed titration behavior were obtained. Both calculations also predicted that the proton uptake by Asp-L213 is low but for different reasons (see ref. [44] for details).

Subsequent calculations have suggested that upon Q_B reduction, both Glu-L212 and Asp-L213 should protonate (at least partially), the exact amount of proton uptake was quite variable and depends on the details of the structure and theoretical treatment [19,21,22–25,27,39,123]. Alexov and Gunner [19] used a multiconformation continuum electrostatic method to calculate the free energy of ET from Q_A^- to Q_B from pH 5 to pH 11 as well as the proton uptake that occurs on the formation of different redox states of the RC. They calculated that between pH 7 and pH 9 the cluster of interacting residues L210, L213, and L212 has a single negative charge (on Asp-L213) in the ground state, Glu-L212 being protonated at physiological pH in the neutral Q_B state. Both Asp-L213 and Glu-L212 would be protonated in the Q_B^- state. In the Q_B^- state, the cluster still has one negative charge, now on the more distant Asp-L210, i.e., there is a shift of a proton from Asp-L210 to Asp-L213. The calculated proton binding agreed reasonably well with experiment (proton uptake measurements) but disagreed with steady-state FTIR results (no observation of proton uptake by Asp-L213 and of deprotonation of Asp-L210, but identification of protonation of Glu-L212, see Section 4). The discrepancy could be caused by a protein rearrangement that was not included in the model [19]. Furthermore, it became difficult to rationalize the calculated protonation changes with the early interpretation of kinetic results [51–53]. However, the conclusions of the calculations on the wild type RC were partially confirmed by computational analysis of mutant RCs from *Rb. sphaeroides* and *Rb. capsulatus* at L212 and L213 positions [20]. Good agreement was found at neutral pH but the calculations on mutants fail to reproduce the pH independence of the free energy in the high pH region of the Gln- and Ala-L212 mutant RCs. It should be also noticed that the authors use the coordinates of the *Rb. sphaeroides* RC for calculations on *Rb. capsulatus* mutant RCs as no structure is available for the *Rb. capsulatus* RC.

Molecular dynamics simulations of Q_B binding in native *Rb. sphaeroides* RCs also suggest changes of the Glu-L212/Asp-L213 protonation states upon ET. Both residues will be protonated in the Q_B^- state while in the Q_B neutral state these calculations are more consistent with either both residues being ionized or Glu-L212 being protonated and Asp-L213 being ionized [22,23]. In 2000, Knapp and coll., [21] calculated the protonation pattern of the titrable groups of the *Rb. sphaeroides* RC in the dark-adapted and light-exposed X-ray structures [36]. They obtained a protonation change of Glu-L212 of 0.2–0.7 H^+ depending whether the conformational transition between the ET inactive conformation (dark-adapted) and ET active conformation (light-adapted) was included (0.7 H^+) or not (0.2 H^+). In contrast to the data from Alexov and Gunner [19], Asp-L210 was found to be always unprotonated. Asp-L213 takes up 0.5 H^+ when Glu-L212 is mostly protonated in both Q_B and Q_B^- states. Asp-L213 is mostly protonated in both states when Glu-L212 takes up 0.7 H^+, i.e., when the conformational transition is included in the comparison. In a subsequent calculation [24], the values of the one-electron redox potentials for Q_A and Q_B were calculated as a function of the charge states of Asp-L213 and Glu-L212 at pH 7, and reciprocally the protonation states of these two residues was studied as a function of the charge state of the quinones. The redox potential of Q_B exhibits a strong dependence on the charge states of Glu-L212 and Asp-L213. To obtain agreement with the measured value of $E_m(Q_B)$, Asp-L213 has to be nearly protonated (0.75–1.0) before and after ET from Q_A^- to Q_B, while Glu-L212 changes its protonation state from 0.15 H^+ to fully protonated. The most recent calculations from Knapp and coll., imply full protonation of Glu-L212 upon Q_B^- formation [25,123].

Electrostatic calculations of the pK_a of ionizable groups have been also carried out for the RC of *B. viridis* [16–18,124]. It should be

noticed that measurement of proton uptake in response to Q_A/Q_B reduction is difficult in the RC of *B. viridis* because the flash-induced proton binding by the quinone is overlapped by concomitant proton release due to the oxidation of the tightly bound cytochrome. To our knowledge, only the pH dependence of the proton binding pattern on flash-induced cytochrome$^+$ Q_A^- formation has been reported [116]. In *B. viridis* RC, Lancaster et al., [16] identified three acids (Glu-L212, Glu-H177, and Glu-M234) which forms a strongly interacting cluster that is thus different from that of *Rb. sphaeroides* (Glu-L212, Asp-L213, and Asp-L210). A possible reason for the different composition of the cluster is the difference at positions L213 (Asn in *B. viridis*) and M43 (Asp in *B. viridis* and Asn-M44 in *Rb. sphaeroides*). Note, however, that the suppressor mutation Asn-M44→Asp in *Rb. sphaeroides* restores proton transfer in the Asp-L213→Asn mutant RC [119]. Note also that Asp-L210 in *Rb. sphaeroides* is changed to Glu in *B. viridis*. In addition, Glu-L212 was calculated to be more protonated at high pH than at low pH values in *B. viridis*. The net proton uptake coupled to the reduction of Q_B by the Glu cluster is ~0.5 H^+ at pH 7, which is approximately divided among the three residues [16]. In Rabenstein et al., [17,18], Glu-H177 has the largest contribution to the proton uptake (~0.6 H^+) and Glu-L212 does not contribute significantly at pH 7.5 since it is almost completely protonated for all redox states of Q_A and Q_B. Thus, all calculations show that there is little proton uptake by Glu-L212 in *B. viridis*. However, these calculations were not in agreement with FTIR spectroscopy which shows no proton uptake by carboxylic acid residues in the 1770–1700 cm^{-1} domain of the Q_B^-/Q_B spectrum of *B. viridis* [125]. Early FTIR investigations of Q_B reduction in *B. viridis* RCs were interpreted in terms of a small proton release of at most ~0.1 H^+/Q_B^- by a carboxylic group [125,126]. Later, it has been proposed that the small signals observed in the 1770–1700 cm^{-1} domain of the Q_B^-/Q_B spectrum of *B. viridis* are largely dominated by contributions from the electrostatic response of the 10a-ester C=O of H_A and H_B [127]. Therefore, although Glu-L212 is present in the Q_B environment of both *B. viridis* and *Rb. sphaeroides* RCs, it is worth noting that this residue appears to protonate upon Q_B reduction only in *Rb. sphaeroides*.

4. FTIR difference spectroscopy of Q_B reduction in native and mutant RCs

A direct experimental method for probing changes of protonation states and/or environment of Asp and Glu residues upon photo- or redox-induced reactions is provided by IR difference spectroscopy. Light-induced FTIR absorption changes associated with the photoreduction of Q_B in native and mutant RCs have been monitored in order to investigate the protonation state of a number of carboxylic acid residues near Q_B. In contrast to the different approaches described in the previous sections the results of which have led to conclusions that have vastly varied over the last 15 years, FTIR studies of native and mutant RCs have consistently given the same set of results, i.e., in the native RC from *Rb. sphaeroides* and *Rb. capsulatus* (i) there is a fraction δ of RCs having Glu-L212 ionized [δ(COO^-)] in the Q_B ground state, (ii) Glu-L212 participates directly to proton uptake upon Q_B photoreduction, and (iii) no signal from any other carboxylic acid was observed:

$$Q_A^-Q_B - -\text{Glu-L212-}\delta(COO^-) + \delta H^+ \rightarrow Q_A Q_B^- - -\text{Glu-L212-COOH} \quad (1)$$

4.1. The C=O stretching IR region of carboxylic amino acids

The C=O stretching mode from the COOH side chain group of protonated carboxylic acid residues (Asp and Glu) is found in the 1770–1700 cm^{-1} spectral domain [42,43]. Its IR frequency depends on the hydrogen-bonding strength of the C=O···H bond [128] and the local environment of this group such as solvent polarity and other electrostatic interactions [129]. On the other hand, the carboxylate (COO^-) modes are expected in the 1580–1555 cm^{-1} (ν_{as}) and ~1400 cm^{-1} (ν_s) spectral ranges [128] where, however, other protein/cofactor modes also contribute and overlap.

Carboxylic acid residues can undergo several types of changes upon photoactivation/redox changes, and each type has a typical FTIR difference spectrum. Protonation (deprotonation) gives rise to a single positive (negative) band. A change of environment or of the hydrogen bonding of a protonated carboxylic group would appear as a differential (S-shaped) signal. An internal proton transfer between two residues would result in a positive and a negative signal provided that the carboxylic groups involved exhibit well-separated COOH modes. Furthermore, the C=O IR stretching mode is sensitive to $^1H/^2H$ isotopic exchange and the major effect is the downshift in solution of the deuterated carboxylic band by up to 10–15 cm^{-1} [130]. The shift is caused by the uncoupling of the O–^2H mode from the C–O mode in the COO^2H group [45].

Changes of carboxylic acid bands in IR difference spectra have been first observed in the bacteriorhodopsin/rhodopsin membrane proteins upon their photochemical cycle [42,43,130–133]. In 1985, we initiated in our laboratory at Saclay the study of ET reactions in the bacterial RC by light-induced FTIR difference spectroscopy in collaboration with Werner Mäntele [134–137]. Electrochemically-induced FTIR spectroscopy has been further applied to analyze the redox changes of the cytochrome *c* [138] and of isolated cofactors, e.g., bacteriochlorophylls [135] and quinones [139,140]. These two different approaches have been extensively used for the past years to study a wide range of membrane and soluble proteins.

The assignment of an IR band to the protonation/deprotonation of a specific carboxylic acid residue is based on changes in the FTIR difference spectrum upon $^1H/^2H$ isotopic exchange and on the effects of site-directed mutations. However, the sensitivity of a carboxylic C=O mode to $^1H/^2H$ isotopic exchange implies that the residue is accessible to the solvent.

4.2. The Q_B^-/Q_B FTIR spectra of the native bacterial RC in ^1H_2O and ^2H_2O

Fig. 4 shows the Q_B^-/Q_B spectra of native RCs from *Rb. sphaeroides* obtained at neutral pH after a saturating laser flash under steady-state conditions in ^1H_2O (a) and ^2H_2O (b). In ^1H_2O, the Q_B^- minus Q_B FTIR difference spectrum displays a main positive band at 1728 cm^{-1} lying in the typical absorption region of COOH groups from Asp and Glu amino acids, as well as small signals at 1740 cm^{-1} (negative) and 1706 cm^{-1} (positive) (Fig. 4a) [44,45]. The increase of absorption at 1728 cm^{-1} (without a negative counterpart) is indicative of an increase of protonation of an Asp or Glu side chain concomitant with the reduction of Q_B. From IR studies of model compounds in ^1H_2O and in ^2H_2O [130,141–143], aspartic and glutamic acids exhibit a band in ^1H_2O at ~1717 and 1712 cm^{-1}, respectively, and in ^2H_2O at ~1712 and 1706 cm^{-1}, respectively.

The positive peak at 1728 cm^{-1} (Fig. 4a) has its amplitude reduced in ^2H_2O and a new signal appears at 1717 cm^{-1} (Fig. 4b). The 1740 cm^{-1} and 1706 cm^{-1} signals are not significantly affected in ^2H_2O. The changes in ^2H_2O are best seen in the double-difference spectra calculated between Q_B^-/Q_B spectra obtained in ^1H_2O and ^2H_2O (^1H_2O minus ^2H_2O). In these double-difference spectra, only the residues affected by the photoreduction of Q_B and sensitive to $^1H/^2H$ exchange will give rise to differential and/or shifted bands. Fig. 4c displays the corresponding double-difference spectra in the 1770–1700 cm^{-1} region. In particular, it shows a positive peak at 1728 cm^{-1} and a negative peak at 1717 cm^{-1} [44]. This ~10 cm^{-1} downshift is typical of a protonated Asp or Glu carboxylic group exchangeable with the solvent. The smaller amplitude of the peak in ^2H_2O relative to that in ^1H_2O could be explained by a slightly larger distribution of hydrogen bonds in ^2H_2O compared to ^1H_2O, thus leading to a broader apparent

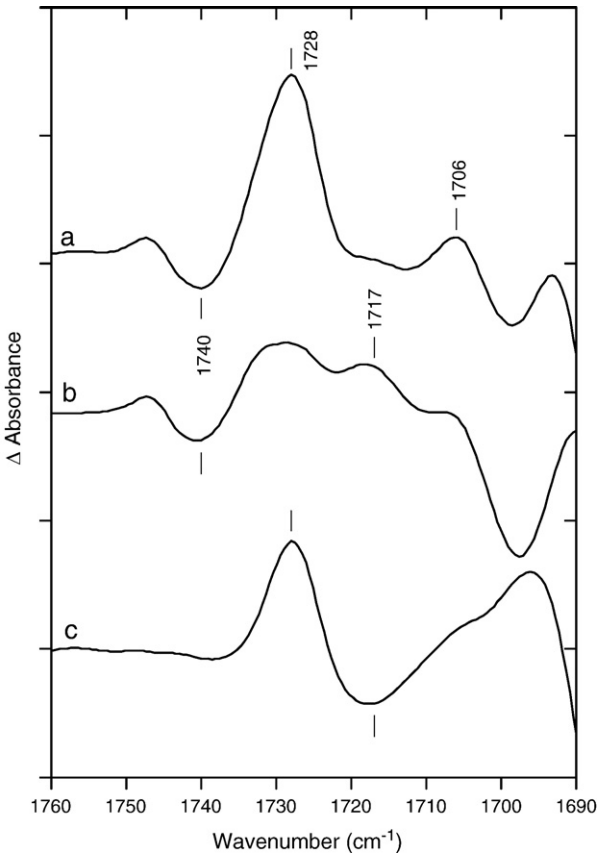

Fig. 4. Light-induced Q_B^-/Q_B FTIR difference spectra in the 1760–1690 cm^{-1} range of native RCs from *Rb. sphaeroides* at pH 7 in (a) ^1H_2O and (b) ^2H_2O. The corresponding calculated double-difference spectrum ^1H_2O minus ^2H_2O is displayed in (c).

band at 1717 cm^{-1} than at 1728 cm^{-1}. Similar IR patterns were also observed in ^1H_2O and ^2H_2O for the carboxylic acid region of the Q_B^-/Q_B spectra of *Rb. capsulatus* RCs [49,50].

4.3. Q_B^-/Q_B FTIR spectra of mutant RCs

In order to identify the 1728 cm^{-1} peak to a specific carboxylic acid of the Q_B pocket, we have investigated the photoreduction of Q_B in a series of mutant RCs of the L and H subunits where individual carboxylic acid groups are replaced with non protonable groups. Owing to the importance of a number of residues near Q_B for high efficiency of coupled electron-proton transfer reactions (Fig. 2), we have studied the photoreduction of Q_B in a series of single mutant RCs at Asp-L213 [44,114,144], Asp-L210 [44,46,48,145], Asp-M17 [46,48], Glu-L212 [44,46,144,146,147], Glu-H173 [47], as well as combinations of these mutations in double and triple mutant RCs [44,46, 144,146,147]. In native RCs, Asp-L210 was suggested to be involved in the Q_B to Q_B^- reaction by electrostatic computations [19,27] and time-resolved FTIR measurements [8,148]; Asp-L210 and Asp-M17 had a synergistic effect on net proton flow through the pathways [149,150]; Glu-H173 had an electrostatic influence on other groups in the pathway [98,103,123,151], in particular Q_B^- and Glu-L212. In general, the carboxylic side chain was changed with the corresponding amide group (Table 1). For the presentation of the data, the mutants are split into three groups. All the mutants of the first group, including native RCs, retain Glu-L212. The second group has Glu replaced with Gln at L212. The third group has Glu and Asp interchanged at the L212 and L213 positions, respectively, and the corresponding data will be described in Section 5.

4.3.1. Mutants retaining Glu-L212

Fig. 5A shows the Q_B^-/Q_B spectra in the 1760–1690 cm^{-1} region of native and several mutant RCs at neutral pH. The main band observed at 1728 cm^{-1} in native RCs is also observed at 1728–1727 cm^{-1} in mutant RCs with Asn-L213 (mutant DN-L213), Gln-H173 (EQ-H173), Asn-M17 (DN-M17), and Asn-L210 (DN-L210). Its amplitude is larger in all these single mutant RCs as well as in the double mutant DN-L210/ DN-M17 (not shown, see [46]). In view of the strong electrostatic interactions expected among many nearby carboxylic acids forming a cluster near Q_B, a remote possibility would be that the 1728 cm^{-1} peak corresponds to protonation distributed over several carboxylic groups in response to Q_B^- formation. However, the ~1728 cm^{-1} band observed in the Q_B^-/Q_B spectra of the first group of mutant RCs is also sensitive to $^1H/^2H$ isotopic exchange and the same frequency downshift by ~10 cm^{-1} in ^2H_2O is observed in the ^1H_2O minus ^2H_2O spectra of all these mutants (Fig. 5B). Thus, the remarkable similarity between the ^1H_2O minus ^2H_2O double-difference spectra of wild type, DN-L213, EQ-H173, DN-M17, and DN-L210 RCs in the 1735–1710 cm^{-1} region (Fig. 5B) provides compelling evidence that a single residue gives rise to the 1728 cm^{-1} signal and is similarly sensitive to $^1H/^2H$ isotopic exchange.

4.3.2. Mutants lacking Glu at L212

In contrast, the Q_B^-/Q_B spectra in ^1H_2O of mutant RCs with Gln at L212 instead of Glu (referred to the second group of mutants in the following) are all drastically modified in the 1735–1720 cm^{-1} region (Fig. 6a–c, see also Fig. 5) compared to all the other spectra described above. There is the conspicuous absence of the 1728 cm^{-1} signal in the single EQ-L212 (Fig. 6a), the double EQ-L212/DN-L210 (Fig. 6b), and the triple EQ-L212/DN-L210/DN-M17 (Fig. 6c) mutant RCs [44–46]. Instead, a small differential signal at 1739(−)/1731(+) cm^{-1} remains and is not significantly sensitive to $^1H/^2H$ isotopic exchange (Fig. 6d–f). It should be emphasized that the three spectra in Fig. 6a–c are very similar, thus suggesting that neither Asp-L210 nor Asp-M17 contributes to the EQ-L212 spectrum. The corresponding double-difference spectra ^1H_2O minus ^2H_2O are displayed on Fig. 6d–f. They are also very similar, showing a very small isotope effect at 1730(+) and 1724(−) cm^{-1} with the amplitude of the signals only marginally larger than the noise level. Consistent with the replacement of Glu-L212 with Ala, the Q_B^-/Q_B spectrum of the double Glu-L212→Ala/Asp-L213→Ala mutant RC of *Rb. sphaeroides* in ^1H_2O lacks the 1728 cm^{-1} band [69]. This band is also absent in the spectrum of the EQ-L212 mutant from *Rb. capsulatus* RCs [49,50] where the remaining differential signal at 1739(−)/1731(+) cm^{-1} shows an amplitude several times larger than in the corresponding *Rb. sphaeroides* mutant.

4.4. Glu-212 is the only carboxylic acid residue that undergoes protonation changes in response to the formation of Q_B^- in native RCs from Rb. sphaeroides

The 1728 cm^{-1} FTIR band is observed in all mutant (and native) *Rb. sphaeroides* and *Rb. capsulatus* RCs which have Glu at L212 and is absent in all mutant RCs lacking Glu at L212. The band is shifted to 1717 cm^{-1} in ^2H_2O. The similarity of the 1728 cm^{-1} (^1H_2O) and 1717 cm^{-1} (^2H_2O) bands in the first group of mutants and in the native RCs (Fig. 5) indicates that the carboxylic acid band at 1728 cm^{-1} in these mutants can be attributed to protonation of Glu-L212 [44–47]. Thus, the positive signal at 1728 cm^{-1} was attributed to substoichiometric proton uptake by Glu-L212 upon Q_B^- formation, based on its absence when Glu-L212 was replaced with Gln [44–47,114,146]. It was concluded that at pH 7 Glu-L212 is at least partially ionized in the Q_B ground state and becomes more protonated upon Q_B photoreduction. This result was not consistent with the assignment of a high pK_a value (9.5) to Glu-L212 [13,51,53,57,58]. In agreement with the steady-state FTIR data, the $P^+Q_A^-Q_B$ to $P^+Q_AQ_B^-$ transition analyzed by kinetic IR spectroscopy with μs time resolution [152] showed that a transient

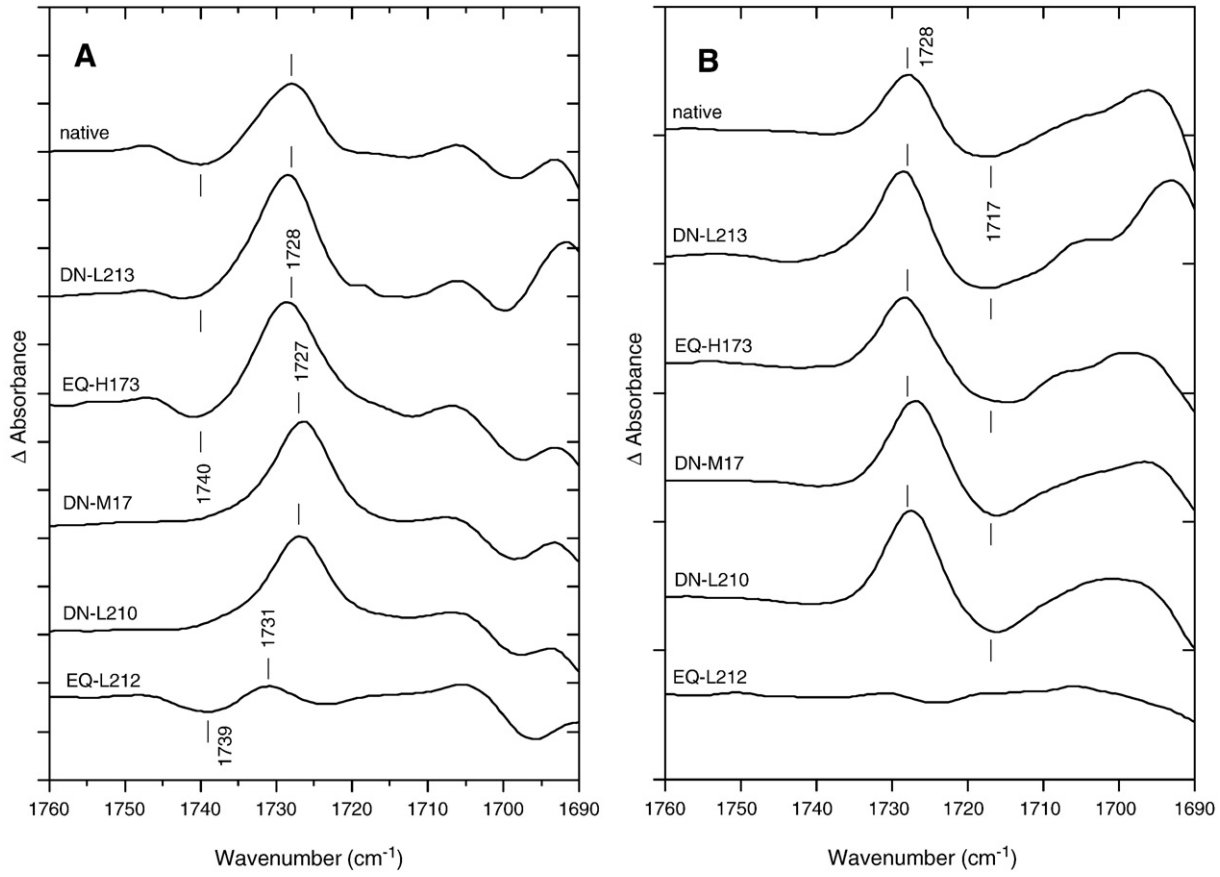

Fig. 5. (A) Comparison of the 1760–1690 cm^{-1} spectral region of the Q_B^-/Q_B spectra of native and mutant (DN-L213, EQ-H173, DN-M17, DN-L210, and EQ-L212) RCs from *Rb. sphaeroides* in ^1H_2O at pH 7. (B) Corresponding calculated double-difference spectra ^1H_2O minus ^2H_2O.

signal monitored at 1725 cm^{-1} in native RCs is absent in EQ-L212 [45,153]. This signal was assigned to the protonation of Glu-L212. A crude estimation of the proton uptake by Glu-L212 has been performed on the basis of molar extinction coefficients and half-widths for COOH [139] and semiquinone [142] bands and has been detailed in [44,45]. The integrated intensity of the 1728 cm^{-1} band would correspond to a proton uptake by Glu-L212 upon Q_B^- formation of 0.3–0.4 H^+in native RCs. From kinetic IR studies on native RCs, a value of 0.3–0.6 H^+/Q_B^- has been reported [45]. The main sources of uncertainty have been discussed in [44].

4.5. Protonation state of Asp-L213, Asp-L210, Asp-M17, and Glu-H173 in the Q_B ground state of native RCs from Rb. sphaeroides

In mutant RCs where Asp-L213 is changed to neutral residue (e.g., Asn, Leu, Ser, or His) the amplitude of the 1728 cm^{-1} band was increased [44, 114] and similarly to native RCs, the band was shifted down by ~10 cm^{-1} in ^2H_2O. The 1728 cm^{-1} signal is also seen in revertants of the Asp-L213→Asn mutant containing second-site suppressor mutations and is similarly sensitive to $^1H/^2H$ isotope exchange [154]. More generally, Q_B^-/Q_B spectra obtained from mutant RCs substituted with Asn or Gln at either one of the L213 [44,114], L210 [44,46,48], M17 [46,48], or H173 [47] sites show that there is an increase of the amplitude of the 1728 cm^{-1} band with respect to that in native RCs, e.g., ~60% in DN-L213, ~50% in EQ-H173, 40% in DN-M17, and ~30% in DN-L210 RCs (Fig. 5A). Note that the amplitude of the 1728 cm^{-1} signal in the Asp-L213→Glu RC [144] as well as in the Glu-H173→Asp RC [47] was comparable to the one observed in native RCs. All these data emphasize the sensitivity of Glu-L212 to the local electrostatic environment. Moreover, in Q_B^-/Q_B spectra of all the mutants of the first group (see Section 4.3.1), there are no new bands in the 1770–1700 cm^{-1} region that could be due to a protonated carboxylic acid. Thus, it appears that in the Q_B^-/Q_B difference spectra of native RCs at neutral pH there is no significant contribution of either Asp-L213, Asp-L210, Asp-M17, or Glu-H173 to the 1770–1700 cm^{-1} carboxylic acid region.

The larger amplitude of the 1728 cm^{-1} signal in the spectra of the DN-L213, EQ-H173, DN-M17, and DN-L210 mutants (Fig. 5A) is attributed to the replacement of a negatively charged Asp or Glu in native RCs with a neutral Asn or Gln side chain. The removal of a negatively charged Asp-L213, Asp-L210, Asp-M17, or Glu-H173 would stabilize the ionized form of Glu-L212. In these mutant RCs, the equilibrium fraction of RCs having Glu-L212 ionized in the Q_B ground state is therefore increased (larger δ in Eq. (1)), leading to an increased proton uptake by this residue. This implies that, in native RCs at neutral pH, the residues Asp-L213, Asp-L210, Asp-M17, and Glu-H173 are mostly ionized in both Q_B and Q_B^- (in agreement with kinetic ET results [51–54,149–151]) and do not significantly change their protonation state upon Q_B^- formation.

The small negative signal observed at 1740 cm^{-1} in native RCs is not seen in DN-L210, DN-M17 (Fig. 5A), and DN-L210/DN-M17 [46] RCs, but it is present in the mutants containing the single EQ-L212 mutation (Fig. 6a–c), the double mutations EQ-L212/DN-L213 [44], and EQ-L212/DN-L210 [46] as well as in the triple mutant EQ-L212/DN-L210/DN-M17 [46]. In all the mutants containing the Gln-L212 mutation (Fig. 6a-c) the small differential signal at ~1739/1731 cm^{-1} in ^1H_2O is not significantly sensitive to $^1H/^2H$ exchange. It is therefore not assigned to a perturbation of carboxylic acid group(s) as discussed in [44,46] and is more likely to reflect an electrochromic shift of the 10a-ester carbonyl of H_A and H_B [127,160] which would not occur in

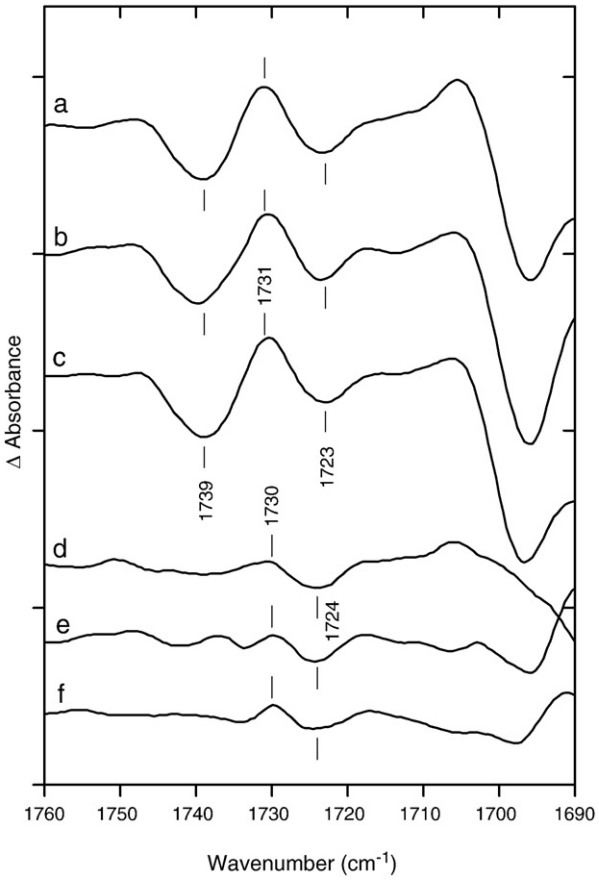

Fig. 6. Comparison of the 1760–1690 cm^{-1} spectral region of the Q_B^-/Q_B spectra of mutant RCs from *Rb. sphaeroides* in ^1H_2O at pH 8. (a) EQ-L212, (b) EQ-L212/DN-L210, (c) EQ-L212/DN-L210/DN-M17. (d, e, f) Corresponding calculated double-difference spectra ^1H_2O minus ^2H_2O.

the DN-L210, DN-M17, and DN-L210/DN-M17 RCs. It is worth noting that in the three latter mutants a differential signal at ~1666(+)/1657 (−) cm^{-1} assigned to a backbone change takes place [46]. Reciprocally, no equivalent backbone signal was observed in the double EQ-L212/DN-L210 and triple EQ-L212/DN-L210/DN-M17 mutant RCs. One interpretation of these results is that the electrostatic environment of the 10a-ester carbonyl of H_A and H_B could be modulated by the dipole involved in the observed backbone change.

5. New strategies to probe protonation patterns of internal carboxylic groups in reaction centers

Despite the abundance of carboxylic acids forming a cluster located structurally in the vicinity of Q_B and the expected strong electrostatic interactions between them [14,15,19,36], the FTIR data described in the previous section show that at neutral pH, no signal from any carboxylic acid other than Glu-L212 could be identified in the Q_B^-/Q_B steady-state spectra of native or of a number of mutant RCs [40,44–50,114]. In particular, no signal for Asp-L213 was found despite its position close to Q_B and its importance for proton conduction toward reduced Q_B in the second ET step [52–54]. Comparison of kinetics studies of the first ET reaction in native and DN-L213 RCs have suggested that the pK_a of Asp-L213 is less than 5 [52–54].

Therefore, FTIR studies of native RCs at lower pH (e.g., below pH 5) and higher pH (above pH 9.5) may reveal protonation events upon Q_B^- formation assignable to Asp-L213 or any other carboxylic groups. We have thus studied the effect of pH on the carboxylic IR region of the Q_B^-/Q_B spectrum of native RCs. In a second approach, we have probed new protonation patterns of internal carboxylic groups in the RC from *Rb. sphaeroides* by studying a third group of mutants [155] which have Glu and Asp interchanged at the L212 and L213 positions and their corresponding amide analogues [146,147].

5.1. pH dependence of IR carboxylic acid signals upon Q_B^- formation in native RCs from Rb. sphaeroides

When individual titrable groups interact with each other, e.g., in a cluster of polar and acid residues, their pH dependence can be much more complex than that of an individual group. The relative contribution of individual groups to the FTIR spectra is weighted by the intrinsic pK_a of the carboxylic acids and the pH of the measurement. Upon Q_B^- formation, the change of protonation state of a given carboxylic acid is determined by its change of pK_a between the state Q_B and the state Q_B^-.

The Q_B^-/Q_B spectra of native RCs were obtained at various pH values between 4 and 11. At all pH values, the region of protonated carboxylic groups is characterized by a main positive band at ~1728 cm^{-1} in ^1H_2O. Since spectra obtained at pH 5.8, 7, 8, and 9.5 (data not shown) were identical in the carboxylic acid region, Fig. 7A only shows the 1760–1690 cm^{-1} region of Q_B^-/Q_B spectra obtained at pH 4 (a), 7 (b), and 11 (c) in ^1H_2O (blue) and ^2H_2O (red). At pH 7 and 4, the band at ~1728 cm^{-1} in ^1H_2O is shifted to ~1717 cm^{-1} in ^2H_2O. At pH 11, the band peaks at 1727 cm^{-1} in ^1H_2O and at 1715 cm^{-1} in ^2H_2O. Moreover, comparison of the double-difference spectra ^1H_2O minus ^2H_2O (Fig. 7B) shows similar qualitative IR patterns at pH 4, 7, and 11 between 1735 and 1700 cm^{-1}. These identical $^1H/^2H$ IR patterns observed for the carboxylic acid(s) in the native RC upon Q_B^- formation at different pH values demonstrate the involvement of the same titrating group(s) over the whole pH range investigated.

Furthermore, an increase in the intensity of the band at 1728 cm^{-1}, i.e., of the proton uptake by Glu-L212, is observed at both pH 4 (~40%) and pH 11 (~30%). The amplitude of the negative signal at 1740 cm^{-1} is also larger at pH 4 than at pH 7 whereas this signal is not seen at pH 11 (Fig. 7Ac), as previously observed [156]. We note that the absence of the 1740 cm^{-1} signal at pH 11 is correlated with the presence of a backbone signal at 1666/1657 cm^{-1} (data not shown), similarly to what was observed in DN-L210, DN-M17, and DN-L210/DN-M17 [46] mutant RCs compared to native RCs. As already discussed in this work, the 1740 cm^{-1} signal the intensity of which varies under different conditions (pH, mutations, bacterial species) is not assigned to a change of a carboxylic acid. Furthermore, kinetic IR studies (μs time resolution) of the $Q_A^-Q_B$ to $Q_AQ_B^-$ ET reaction in native RCs [45] indicated that the amplitude of the slow kinetic component of the 1725 cm^{-1} signal decreased between pH 5.5 and pH 6.3 and then it gradually increased up to pH 10, suggesting a gradually increasing fraction of ionized Glu-L212 (δ-COO^-) between pH 6.3 and pH 10. The latter set of data are in agreement neither with the steady-state FTIR results (Fig. 7)[2] nor with a pK_a of 9.5 for Glu-L212 [13,51,53,57,58].

5.2. What could be the pK$_a$ of Glu-L212 in the native reaction center?

In native RCs, it thus appears that the major contribution to proton uptake at all pH values is the protonation of Glu-L212 due to a strong electrostatic coupling between the ionized Glu-L212 and Q_B^-. One main result of the FTIR pH (and mutant) studies is that Glu-L212 serves as an electrostatic nucleus for proton uptake on the first ET step. Glu-L212 has also an important role on the second proton-coupled ET step which is to provide rapidly a proton to the doubly reduced Q_BH^- species to form the quinol that is subsequently released from the Q_B

[2] It should be emphasized that in kinetic IR data reported in ref. 45, the data point at pH 6.3 is somewhat anomalous and, without it, the trend in the amplitude of the slow phase at 1725 cm^{-1} as a function of pH is not inconsistent with the steady-state FTIR data obtained at different pH values (Fig. 7).

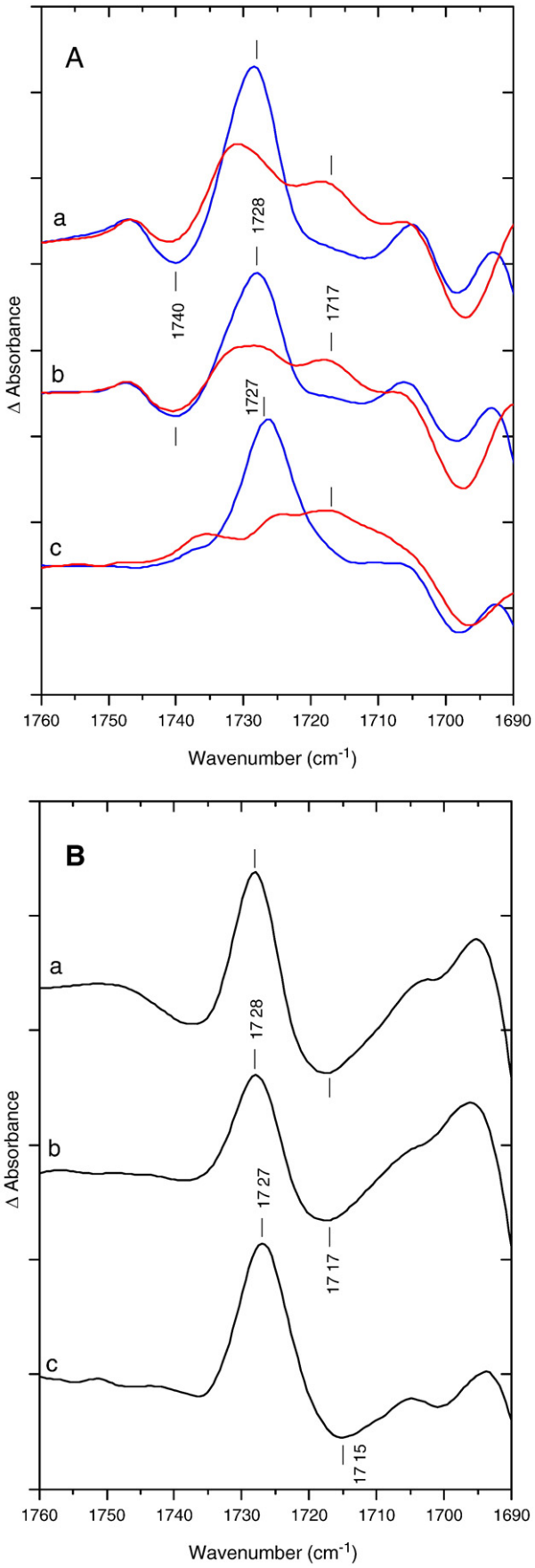

Fig. 7. (A) Effect of pH on the 1760–1690 cm^{-1} spectral region of the Q_B^-/Q_B spectra of native RCs from *Rb. sphaeroides* in ^1H_2O (blue) and ^2H_2O (red) at pH 4 (a), pH 7 (b), and pH 11 (c). (B) Corresponding calculated double-difference spectra ^1H_2O minus ^2H_2O at pH 4 (a), pH 7 (b), and pH 11 (c).

binding site. Another important FTIR result is that no signal from any other carboxylic acid could be identified in the Q_B^-/Q_B spectra obtained at different pH values in native RCs (Fig. 7) but also in the single EQ-L212 and DN-L213 mutants [[157], and E. Nabedryk, J. Breton, M.L. Paddock, M.Y. Okamura, unpublished results], in particular no signal for Asp-L213 was found at any pH values investigated.

What could be the pK_a of Glu-L212 in native RCs? Both steady-state FTIR data [44,46–48,114] and kinetic IR studies [45] are inconsistent with a pK_a of 9.5 for Glu-L212 [13,51,53,57,58]. The present steady-state FTIR data show that Glu-L212 becomes protonated upon Q_B^- formation at all pH values, with an increase of the protonation state at low (pH 4) and high (pH 11) pH. A possible interpretation for this very unusual behavior for a carboxylic acid would be that two populations of Glu-L212 coexist in the RC: one would have a pK_a<4 whereas the other would have a pK_a>11. Such a model has been also proposed from the study of the electrogenicity of the $Q_A^-Q_B$ to $Q_AQ_B^-$ transition in *Rb. sphaeroides* RCs [61,62].

5.3. Identification of a novel protonation pattern for carboxylic groups upon Q_B reduction in the Asp-L212/Glu-L213 swap mutant RC

In an attempt to uncover the reason behind the lack of involvement of carboxylic signals other than that of Glu-L212 in native RCs upon Q_B reduction, a novel strategy was recently developed to probe new protonation patterns of internal carboxylic groups in the RC from *Rb. sphaeroides*. The possibility of changing the microscopic electrostatic environment near Q_B without perturbing the overall macroscopic environment offers a novel way to probe protonation patterns of internal carboxylic acids. This was accomplished by interchanging Asp and Glu at L212 and L213 [155]. Previous kinetic measurements of ET rates in the Asp-L212/Glu-L213 mutant RC suggested that the overall electrostatic environment near Q_B was similar to the native RC, but there was a difference in the microscopic electrostatic environment attributed to differences in the state of ionization of Asp and Glu at either L212 or L213 [155]. Recently, this mutant became the basis of a FTIR study that led to the identification of a novel protonation pattern of carboxylic acids near Q_B [146]. Fig. 8 displays Q_B^-/Q_B spectra of the Asp-L212/Glu-L213 mutant RC (henceforth referred to as the swap mutant) and its amide analogues in ^1H_2O (A) and ^2H_2O (B). The swap mutant exhibited several previously unobserved features in the 1785–1685 cm^{-1} IR region of protonated carboxylic acids [146]. Compared with the single prominent positive peak observed at 1728 cm^{-1} in the native RC (Fig. 8Aa), a broad positive band at 1752–1747 cm^{-1} was revealed in the Q_B^-/Q_B spectrum of the swap mutant together with positive signals at 1731 and 1705 cm^{-1} and a new broad negative feature at 1765 cm^{-1} (Fig. 8Ab). All these signals were sensitive to $^1H/^2H$ isotopic exchange, although only part of the 1705 cm^{-1} signal was affected. This indicates that the reduction of Q_B in the swap mutant results in the change of protonation state and/or environment of several (at least four) individual carboxylic acids [146]. The double-difference spectra ^1H_2O minus ^2H_2O have been reported and discussed in [146].

5.4. Assignment of carboxylic C=O modes of Glu-L213 and Asp-L212 in the swap mutant

The broad band at 1752–1747 cm^{-1} was assigned to an increase of protonation in response to Q_B reduction of Glu-L213 (at 1752 cm^{-1}) and Asp-L212 (at 1747 cm^{-1}), based on the effect of replacing these residues with their amide analogs [146]. The Q_B^-/Q_B spectrum in ^1H_2O of the Asp-L212/Gln-L213 RC (Fig. 8Ac) shows the absence of the

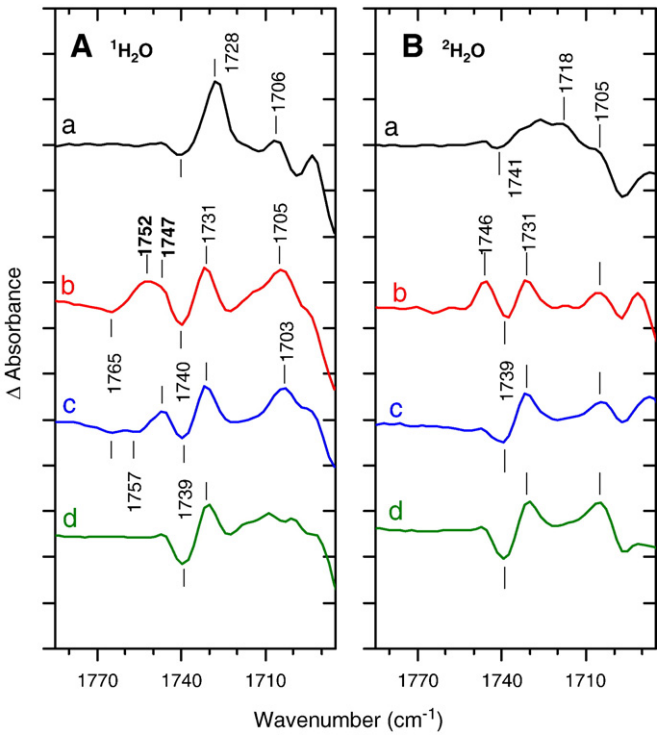

Fig. 8. Comparison of the 1785–1685 cm^{-1} spectral region at pH 7 of the Q_B^-/Q_B spectra in ^1H_2O (A) and ^2H_2O (B) for (a) native, (b), Asp-L212/Glu-L213, (c) Asp-L212/Gln-L213, and (d) Asn-L212/Glu-L213 RCs.

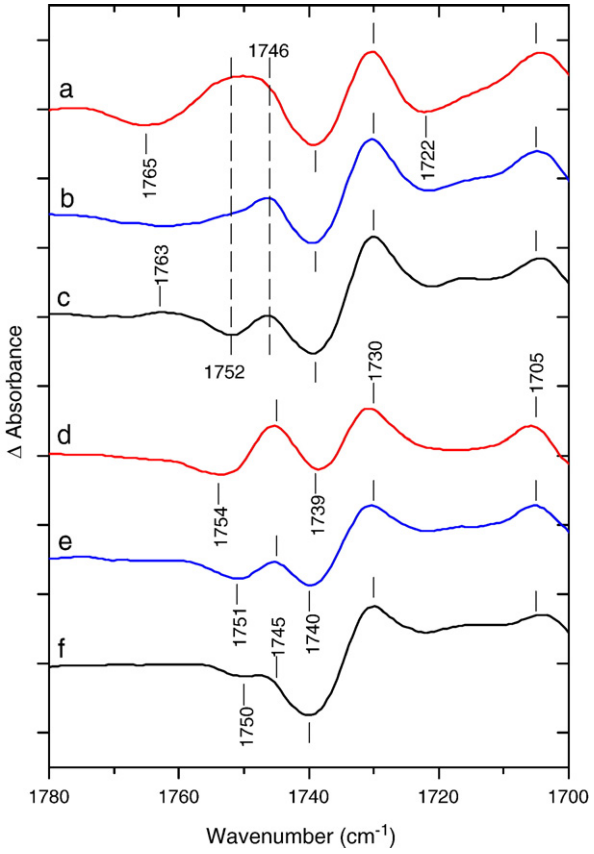

Fig. 9. Effect of pH on the 1780–1700 cm^{-1} spectral region of the Q_B^-/Q_B spectra of the Asp-L212/Glu-L213 swap mutant RCs in ^1H_2O at pH 8 (a), pH 5 (b) and pH 4 (c) and in ^2H_2O at pD 8 (d), pD 5 (e), and pD 4 (f).

highest frequency peak at 1752 cm^{-1} although the lower peak at 1747 cm^{-1}, which is sensitive to $^1H/^2H$ exchange (Fig. 8Bc), is still present. Thus, the 1752 cm^{-1} peak was assigned to the partial protonation of Glu-L213 upon Q_B^- formation. In the Q_B^-/Q_B spectrum in ^1H_2O of the Asn-L212/Glu-L213 RC (Fig. 8Ad), both the 1752 and 1747 cm^{-1} peaks are absent. The 1747 cm^{-1} signal, which is observed in both Asp-L212/Glu-L213 and Asp-L212/Gln-L213 RCs, was therefore assigned to partial protonation of Asp-L212 upon Q_B reduction.

These results show that the protonation patterns of carboxylic acids and hence their resultant FTIR signatures are very sensitive to the environment and can be strongly affected by what is often considered fairly conservative amino acid replacements (Asp with Glu and Glu with Asp). It was concluded that the swap mutations at L212 and L213 influence a cluster of carboxylic acids larger than the L212/L213 acid pair [146]. In the swap mutant, there is proton sharing amongst a cluster of carboxylic acids in a system very similar to the native RC, which differs in the absorption frequency of protonating carboxylic acids and in the extent of proton sharing. Understanding this difference between native and swap mutant RCs is probably essential for elucidating proton-coupled ET reactions within the bacterial RC.

5.5. pH dependence of IR carboxylic acid signals in the swap mutant upon Q_B^- formation

Since several carboxylic acids participate to proton sharing in the swap mutant, pH was used to help deconvolute the spectra. In contrast to native RCs, large pH-dependent changes were observed in the 1780–1700 cm^{-1} absorption range of the Q_B^-/Q_B FTIR difference spectrum of the Asp-L212/Glu-L213 swap mutant at pH values ranging from 8 to 4 [147]. Fig. 9 shows the Q_B^-/Q_B spectra of the swap mutant obtained at pH 8, 5, and 4 in ^1H_2O (a–c) and ^2H_2O (d–f). The protonation pattern obtained at pH 10 (E. Nabedryk, unpublished data) was similar to the one observed at pH 8 and pH 7 indicating pK_a (Q_B^-)>10. The Q_B^-/Q_B spectra (Fig. 9) clearly showed that the two underlying components of the broad band centered around 1750 cm^{-1} have different pH sensitivities. This difference resulted in a decrease of the highest frequency component (at 1752 cm^{-1}) at pH 5 (Fig. 9b) whereas the lowest frequency component (at 1746 cm^{-1}) remained present even at pH 4 (Fig. 9c).

The specific effects of pH on the protonation pattern of the carboxylic acids in the Q_B^-/Q_B spectum of the swap mutant are best visualized in the double-difference spectra calculated from the individual Q_B^-/Q_B spectra recorded at a given pH in ^1H_2O and in ^2H_2O. Fig. 10 shows the calculated double-difference spectra ^1H_2O

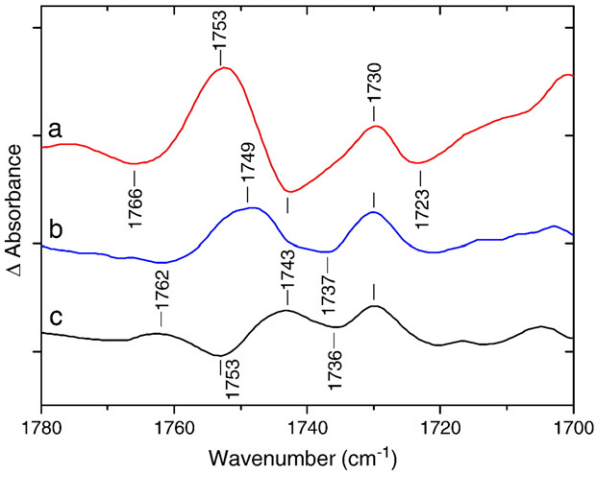

Fig. 10. Calculated double-difference spectra ^1H_2O minus ^2H_2O for the Asp-L212/Glu-L213 swap mutant RCs at pH 8 (a), pH 5 (b), and pH 4 (c).

minus ^2H_2O at pH 8 (a), pH 5 (b), and pH 4 (c). Apart from a common feature present in all spectra at 1730(+)/~1723(−) cm^{-1}, the calculated spectra reveal several distinct features. The main feature of the ^1H_2O minus ^2H_2O spectrum at pH 8 (Fig. 10a) is a positive peak at 1753 cm^{-1} and a negative band at 1743 cm^{-1}. At pH 5 (Fig. 10b), the double-difference spectrum shows a broad positive band at 1749 cm^{-1} and a broad trough between 1743 and 1737 cm^{-1}. At pH 4 (Fig. 10c), a negative signal appears at 1753 cm^{-1} and a positive one at 1743 cm^{-1}. The shift of the broad band around 1770–1760 cm^{-1} differs at each pH displaying a negative component at 1766 cm^{-1} at pH 8, an almost featureless pattern at pH 5, and a positive broad feature at 1762 cm^{-1} at pH 4. These differences demonstrate that at each pH a unique combination of carboxylic acids contributed to the observed spectra. If all carboxylic groups involved in the Q_B to Q_B^- formation had the same titration pattern with pH, the ^1H_2O minus ^2H_2O spectra obtained at each pH would be identical in shape (as observed in native RCs). Hence, the differences in the spectra of the swap mutant at each pH show that they result from the superposition of peaks from titrating groups having different titration behaviors.

5.6. Assignment of pH-dependent carboxylic acid modes in the swap mutant

The ^1H_2O minus ^2H_2O FTIR fingerprint spectra for the swap mutant (Fig. 10) demonstrate that the pH dependence of proton uptake differs for the two main components of the broad band centered around 1750 cm^{-1}, i.e., for Glu-L213 and Asp-L212, as well as for the small signal at ~1765 cm^{-1} (Fig. 10). The IR data demonstrate that protonation of Glu-L213 occurs at pH 8 and pH 5 but not at pH 4 while that of Asp-L212 occurs over the entire pH range from 8 to 4.

Other unanticipated signals appear in the FTIR spectra of the swap RC, notably at 1730/1723 cm^{-1} (+), near 1765 cm^{-1} (−), and at 1705 cm^{-1} (Figs. 9 and 10). This latter signal does not significantly vary with the pH (Fig. 9). Approximately one third of the 1730/1723 cm^{-1} peak titrated and this signal is likely to originate from changes of a carboxylic acid upon Q_B reduction. The remaining two third was invariant. The negative feature observed at ~1765 cm^{-1} at pH 8 (Fig. 9a) and the positive signal appearing at ~1763 cm^{-1} at pH 4 (Fig. 9c) could reflect either a pH-dependent environmental change of a protonated carboxylic acid or $\delta H^+$of a carboxylic acid, with δH^+ approaching zero at pH 5 (Fig. 9b). These signals are also clearly identified in ^1H_2O minus ^2H_2O spectra (Fig. 10) at pH 8 (negative signal at 1766 cm^{-1}) and pH 4 (positive signal at 1762 cm^{-1}). Because the 1770–1760 cm^{-1} region is flat at pH 7 in the FTIR spectrum of the Asn-L212/Glu-L213 mutant (Fig. 8Ad), the 1765 cm^{-1} signal observed at pH 8 in the swap mutant could be the proton donor to Asp-L212. Since the changes observed in ^2H_2O (at ~1765 and at 1730/1723 cm^{-1}) are very small, they could arise from carboxylic acids located further from Q_B, and hence less perturbed by its reduction. Possible carboxylic acids that are located between the surface of the RC protein and the destination of the protons near L212 and L213 are Asp-L210, Asp-M17, and Glu-H173 (Fig. 2). Further studies involving additional mutations at L210, M17, and H173 in the swap mutant RC background will be necessary to determine the possible contributions of these carboxylic acid(s) to the remaining unassigned signals.

5.7. Why are the native RC and the swap mutant different?

FTIR spectra at different pH values of the swap mutant are rich in information on the behavior of internal carboxylic acids. The observation of several distinct carboxylic bands in the swap mutant indicated that protonation or proton movement occurred amongst several carboxylic acids upon Q_B^- formation. The observation that these carboxylic bands were differentially sensitive to pH changes showed that electrostatic interactions occur between these acids and, in particular, between those at the L212 and L213 sites. Differences in the electrostatic interactions amongst the acids of the cluster near Q_B resulting from the interchange of Glu for Asp at L212 and Asp for Glu at L213 are likely to cause the changes in the FTIR spectra. In this regard, electrostatic calculations of the interactions of carboxylic acids near Q_B in the swap mutant should help to establish the differences in interactions and hence the resultant FTIR spectrum; this is a non-trivial and challenging exercise given the number of titrating groups in close proximity and the unknown position of many internal water molecules [36,37]. In addition, an attractive approach would be to use time-resolved (TR) FTIR spectroscopy [8,148] to follow transient protonation changes of individual carboxylic groups at different pHs. Such an approach should provide detailed information on the molecular mechanism of electron and proton transfer during Q_B photoreduction.

6. Time-resolved FTIR investigation of the $Q_A^-Q_B \rightarrow Q_AQ_B^-$ electron transfer in native and mutant reaction centers

As reported in the previous sections, large amounts of data have been obtained on RCs by static FTIR difference spectroscopy for specific redox states of the two quinone acceptors. Compared to static FTIR difference spectroscopy, TR FTIR difference spectroscopy can monitor transient states of a reaction, revealing for example the reduction of a cofactor and the concomitant protonation of a nearby amino acid residue that might not be detectable in static FTIR difference spectroscopy. Several IR and FTIR kinetic techniques have been applied to the photoreduction of quinones in native RCs and a few mutants from *Rb. sphaeroides*. Light-induced transient spectra $P^+Q_A^-Q_B/PQ_AQ_B$ and $P^+Q_AQ_B^-/PQ_AQ_B$ in native RCs were first investigated by rapid-scan (RS) FTIR difference spectroscopy (time resolution ~25 ms) by virtue of the large differences of the decay time of the $P^+Q_A^-Q_B$ (~100 ms) and $P^+Q_AQ_B^-$ (several seconds) states at 280 K. Upon substracting the large IR contributions of P and P^+states in these spectra, a double-difference spectrum $Q_A^-Q_B/Q_AQ_B^-$ was obtained, allowing for the first time the only contributions of Q_A, Q_A^-, Q_B, and Q_B^- to be revealed [158]. This double-difference spectrum turned out to be very similar to that calculated from the individual Q_A^-/Q_A and Q_B^-/Q_B FTIR difference spectra that were subsequently obtained under steady-state conditions [101]. Transient signals associated with the $Q_A^-Q_B \rightarrow Q_AQ_B^-$ ET reaction were first characterized using tunable IR laser diodes [45,152,153] and later by step-scan FTIR spectroscopy [159]. In the latter case, the reported $Q_A^-Q_B/Q_AQ_B^-$ double-difference spectrum between transient spectra measured at 7 μs and 4.2 ms agreed well with those previously reported for measurements on slower time scales [158,101].

In specific mutant RCs where the first ET reaction is slowed down to the ms time domain, a RS FTIR investigation becomes possible. Mezetti et al., [48] have studied the first ET from Q_A^- to Q_B in native RCs from *Rb. sphaeroides* and in the DN-L210, DN-M17 and DN-L210/DN-M17 mutants. RS spectra show that, within the temporal resolution of the measurement (~25 ms), the time evolution of IR marker bands is the same for oxidation of Q_A^-, reduction of Q_B, and protonation of Glu-L212 in all samples. These findings confirm the model derived from visible spectroscopy that ET and protonation of Glu-L212 are kinetically coupled [108]. However, no other carboxylic acid signal was detected by these RS FTIR studies [48].

In 2003, Rémy and Gerwert [8] proposed a new and unconventional mechanism for the $Q_A^-Q_B \rightarrow Q_AQ_B^-$ ET reaction on the basis of step-scan measurements with high time resolution, from 30 ns to 35 s. They reported that in native RCs Q_B is not reduced by Q_A^- but presumably through a transient intermediary electron carrier X. A subsequent study of the DN-L210 mutant RC [148] where proton and electron transport is slowed down corroborated their initial proposal, i.e., Q_B^- formation precedes Q_A^- oxidation and this phenomenon is more pronounced in the mutant than in the native RC. They assign a signal at 1724–1726 cm^{-1} to protonation of Glu-L212 in the

spectrum of the 150 μs phase and the band continued to increase in the 1.1 ms spectrum. In the spectrum of the 12 μs phase, two bands appeared at 1751 and 1707 cm^{-1} which were assigned to carboxylic signals. No specific assignment to a given carboxylic acid was made for the 1707 cm^{-1} band. It should be emphasized that the ~1706–1707 cm^{-1} signal was also observed in steady-state FTIR difference spectra of Q_B^- formation in native RCs and a number of mutants [44,46,47,49,50,146,147] but it was not assigned to a protonated carboxylic acid. First, it is not significantly sensitive to $^1H/^2H$ isotope exchange [44,45]. Secondly, the positive signal at ~1706 cm^{-1} and a small negative signal at 1698 cm^{-1} are absent in the Q_B^-/Q_B spectrum of the Ala-M149→Trp mutant RC where the cofactor H_B is absent [160]. The differential signal at ~1706(+)/1698(−) cm^{-1} was therefore assigned to an electrostatic influence of Q_B^- on the vibrational mode of the 9-keto C=O of H_B [160].

The 1751 cm^{-1} band was tentatively assigned by Gerwert and coll., [8,148] to the transient protonation of Asp-L210 since in the wild type RC, the band increased by 12 and 150 μs whereas in the DN-L210 mutant a decrease was observed [8,148]. According to Hermes et al., [148] Asp-L210 will be the proton donor to Glu-L212. However, a residual signal was present at 1751 cm^{-1} in the mutant and it was attributed to P^+/P recombination. Indeed, a large contribution from the 10a-ester C=O vibration of P^+dominates the absorption changes at 1751 cm^{-1} in static [134–136] and TR [8,148,158,159] $P^+Q_A^-Q_B/PQ_AQ_B$ and $P^+Q_AQ_B^-/PQ_AQ_B$ FTIR spectra of native and DN-L210 RCs. Moreover, a recent analysis of steady-state Q_A^-/Q_A and Q_B^-/Q_B FTIR spectra of native and DN-L210 RCs [145] shows that the IR signatures of the X^+/X redox pair previously proposed to act as a transient intermediate in the first ET reaction in both native and mutant RCs [8,148] exhibit all the IR fingerprints of the Q_B^-/Q_B couple. Thus, the reaction scheme given in [8,148] as well as the assignment of carboxylic acids at 1751 cm^{-1} and 1707 cm^{-1} should be reconsidered[3] and will deserve further TR FTIR investigations.

7. Perspectives: possible role of water molecule(s) in the proton transfer to reduced Q_B in the native reaction center

In the bacterial RC from *Rb. sphaeroides*, chains of ordered water molecules connecting Q_B to the cytoplasmic surface were observed in the structure of the RC [16,30,36,37,161]. These water clusters are also connected to amino acid residues that are crucial to the protonation of reduced Q_B. In particular, there is a region located between three carboxylic acid groups, i.e., Asp-L210, Asp-L213, and Asp-M17 which could accommodate one or more water molecule(s) (Fig. 2). An interesting possible explanation for the differences between the native and the swap mutant RC is that an internal water molecule may be a proton acceptor functioning preferentially in the native system (in addition to Glu-L212). In bacteriorhodopsin, a different type of photoactive protein that pumps protons across a bacterial membrane, protonation of an internal water molecule was indicated based on electrostatic computations [162] and FTIR measurements [163–165].

The idea that internal water molecules in the vicinity of Q_B may protonate was originally derived from earlier FTIR measurements in the mid IR region between 3000 and 2000 cm^{-1}. In native RCs from *Rb. sphaeroides*, the observation of a broad positive IR continuum around 2600 cm^{-1} in ^1H_2O in the Q_B^-/Q_B steady-state FTIR spectrum suggests the existence of delocalized proton(s) in a highly polarizable hydrogen-bonded network [126]. This band has also been recently observed in slow TR FTIR measurements on the DNL210 mutant RC [148]. Upon $^1H/^2H$ isotopic exchange, the maximum of the band is shifted to ~2080 cm^{-1} (Fig. 11a). In RCs from *B. viridis*, the IR continuum is seen at ~2830 cm^{-1} and ~2180 cm^{-1} in ^1H_2O and ^2H_2O (Fig. 11e), respectively [126]. X-ray models of the two RCs suggest differences in the structural organization of the hydrogen-bonded network (shorter chains in *B. viridis*) whereas several residues in the vicinity of Q_B are not conserved in *B. viridis* (Asp-L213, Asp-M17, Pro-L209, Asn-M44). In addition, FTIR data have shown that protonation of carboxylic acids, in particular of Glu-L212, does not occur in *B. viridis* upon Q_B^- formation [65,125].

According to Zundel [166,167], hydrogen-bonded networks cause intense IR continua in the 3000–2000 cm^{-1} spectral range that are indicative of large proton polarizability due to proton fluctuations within the hydrogen bonds. The continua arise because of strong interactions of these hydrogen bonds with their environment (local electrostatic fields). Indeed, IR spectra of strong acids in ^1H_2O and ^2H_2O display continuous IR absorption extending over more than 1000 cm^{-1} attributed to the excess of proton in the protonated (deuterated) water dimer $^1H_5O_2^+$ ($^2H_5O_2^+$) [166,167,126]. The $H_5O_2^+$ species [168–172] would participate naturally in hydrogen-bonded networks enabling proton transfer.

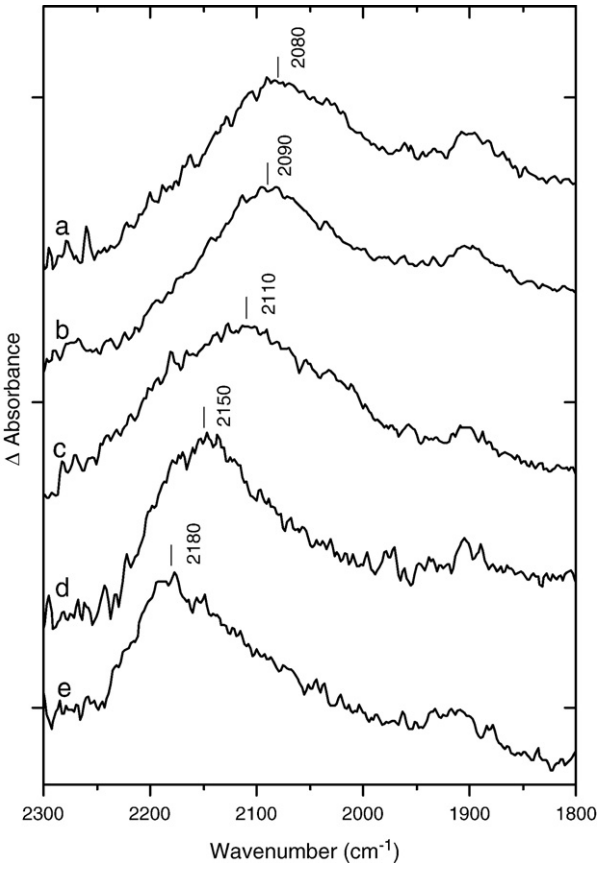

Fig. 11. Comparison of the 2300–1800 cm^{-1} spectral region of the Q_B^-/Q_B spectra in ^2H_2O for native RCs from *Rb. sphaeroides* (a) and *B. viridis* (e) and for mutant RCs from *Rb. sphaeroides*(b–d), pD 7: (b) EQ-L212, (c) DN-L213, (d) ED-L212/DE-L213.

[3] It is important to note that the investigation of the $Q_A^-Q_B$ to $Q_AQ_B^-$ ET by TR IR spectroscopy has to cope with several intrinsic limitations that have been overcome in the generation of the steady-state spectra. The states generated upon excitation of the RCs contain contributions from P and P^+, the IR bands of which are usually of a magnitude larger than those of the neutral and semiquinone forms of Q_A and Q_B. In the case of sub-ms measurements such as kinetic IR and step-scan FTIR spectroscopy, the spectra inevitably contain contributions from the IR bands of P and P^+. Following charge separation between P and Q_A, any relaxation that would occur around P^+ on the time scale of the measurement could therefore be misinterpreted as a change taking place around Q_A^- or Q_B^-. In contrast, the steady-state Q_A^-/Q_A and Q_B^-/Q_B FTIR difference spectra have been generated by using various combinations of reducing agents and mediators, the role of which is to rapidly (compared to the quasi stationary conditions of the measurements) rereduce P^+ after charge separation. The same strategy has been applied in some of the RS measurements [8,48]. However, one should be aware that the time evolution of the formation and decay of the oxidized mediators, which exhibit bands in the mid-IR, might be commensurate with the $Q_A^-Q_B$ to $Q_AQ_B^-$ ET step. As previously discussed in [145], stringent controls have therefore to be carefully applied in both slow and fast TR IR measurements.

In the bacterial RC, the possible relation of the IR continuum band to the acid residues involved in the proton transfer pathway was thus investigated by testing the robustness of this band to different mutations of carboxylic acids in the RC from *Rb. sphaeroides* [173]. Fig. 11 shows the Q_B^-/Q_B spectra in ^2H_2O in the 2300–1800 cm^{-1} spectral range of the native RCs from *Rb. sphaeroides* (a) and *B. viridis* (e), the single EQ-L212 (b) and DN-L213 (c) mutant RCs, and the swap mutant ED-L212/DE-L213 (d). Replacement of an Asp or Glu side chain with the corresponding amide at L212 (Fig. 11b), L210, M17, or H173 has little or no effect on the IR frequency of the IR continuum observed upon Q_B^- formation (E. Nabedryk, J. Breton, upublished data). However, changes were observed in the DN-L213 (Fig. 11c) and in the swap mutant (Fig. 11d) where the broad band is shifted to ~2110 and 2150 cm^{-1}, respectively. Comparable shifts were similarly observed in the Q_B^-/Q_B spectra (data not shown) of the ED-L212/DQ-L213 amide analogue from the swap mutant (at ~2150 cm^{-1}), the DE-L213 (at ~2170 cm^{-1}), and in a revertant of the DN-L213 mutation, i.e., in the double mutant ND-M44/DN-L213 (at ~2150 cm^{-1}). Interestingly, in this latter mutant, the two mutations at L213 and M44 mimic part of the binding site of Q_B in *B. viridis*. For the ED-L212/DE-L213, DE-L213, and ND-M44/DN-L213 mutants, the band is therefore upshifted to ~2830 cm^{-1} in ^1H_2O and ~2150–2170 cm^{-1} in ^2H_2O, and both its shape and its frequency are very comparable to what is observed for *B. viridis* (Fig. 11c). The shift of the IR continuum in the mutant spectra reflects electrostatic effects on the vibrations associated with proton oscillation due to environmental changes and/or local electrical fields.

Since the IR continuum is abolished in none of the mutants and in particular in mutants having Glu-L212 replaced with Gln (Fig. 11b), the presence of the band is not correlated with the localization of the proton on Glu-L212. On the other hand, the band is systematically affected by mutations at L213. We thus propose that the observed changes imply rearrangements of the hydrogen-bonding network close to Q_B. The changes observed in the mutant RCs with respect to native RCs would reflect the specific role of bound protonated water molecule(s) located in the vicinity of Asp-L213, and undergoing hydrogen-bond changes in the network. The proton may fluctuate within two water molecules or between a carboxylic acid and a water molecule. In the native RC from *Rb. sphaeroides*, the protonation of internal water molecule(s) combined with proton uptake by Glu-L212 upon Q_B reduction could help reconcile FTIR data with the large body of contrasting kinetic and proton uptake data available, as recently discussed in [64].

The protonation of water molecule(s) in the native RC from *Rb. sphaeroides* can qualitatively explain the differences observed here between the native and mutant RCs upon Q_B reduction as well as the differences observed between *B. viridis* and *Rb. sphaeroides*. Testing such proposal provides a new challenge for static and TR FTIR difference spectroscopy. Another promising way would be to detect changes of internal water molecules by directly monitoring their localized O–H stretching vibrations in the 3700–2600 cm^{-1} spectral range. Such O–H stretching vibrations have been already observed in the intermediates of the bacteriorhodopsin photocycle and the data are contributing much to the understanding of the photochemical mechanism [[175] and references therein].

Acknowledgements

At the end of our scientific career, we deeply acknowledge all the colleagues and friends, including those at Saclay, for the enlightening discussions and fruitful collaborations. Thanks also to the enthusiastic students and postdocs who have animated life at the laboratory.

For the work described in this review, we would like to thank especially all the laboratories that have provided us with site-directed mutant reaction centers at the Q_B site, notably Mark Paddock and Melvin Okamura together with George Feher for the superb collaboration carried over more than 15 years, and Michael Jones for his sustained interest in FTIR spectroscopy. We have also greatly appreciated our collaboration with Laura Baciou, Pierre Sebban and Deborah Hanson.

References

[1] G. Feher, J.P. Allen, M.Y. Okamura, D.C. Rees, Structure and function of bacterial photosynthetic reaction centres, Nature 339 (1989) 111–116.
[2] M.Y. Okamura, M.L. Paddock, M.S. Graige, G. Feher, Proton and electron transfer in bacterial reaction centers, Biochim. Biophys. Acta 1458 (2000) 148–163.
[3] M.L. Paddock, G. Feher, M.Y. Okamura, Proton transfer pathways and mechanism in bacterial reaction centers, FEBS Lett. 555 (2003) 45–50.
[4] C.A. Wraight, Proton and electron transfer in the acceptor quinone complex of photosynthetic reaction centers from *Rhodobacter sphaeroides*, Front. Biosci. 9 (2004) 309–337.
[5] D.M. Tiede, J. Vàzquez, J. Córdova, P.A. Marone, Time-resolved electrochromism associated with the formation of the quinone anions in the *Rhodobacter sphaeroides* R26 reaction center, Biochemistry 35 (1996) 10763–10775.
[6] J. Li, D. Gilroy, D.M. Tiede, M.R. Gunner, Kinetic phases in the electron transfer from $P^+Q_A^-Q_B$ to $P^+Q_AQ_B^-$ and the associated processes in *Rhodobacter sphaeroides* R-26 reaction centers, Biochemistry 37 (1998) 2818–2829.
[7] J. Li, E. Takahashi, M.R. Gunner, -ΔG°_{AB} and pH dependence of the electron transfer from $P^+Q_A^-Q_B$ to $P^+Q_AQ_B^-$ in *Rhodobacter sphaeroides* reaction centers, Biochemistry 39 (2000) 7445–7454.
[8] A. Remy, K. Gerwert, Coupling of light-induced electron transfer to proton uptake in photosynthesis, Nat. Struct. Biol. 10 (2003) 637–644.
[9] M.S. Graige, G. Feher, M.Y. Okamura, Conformational gating of the electron transfer reaction $Q_A^-Q_B \rightarrow Q_AQ_B^-$ in bacterial reaction centers of *Rhodobacter sphaeroides* determined by a driving force assay, Proc. Natl. Acad. Sci. U. S. A. 95 (1998) 11679–11684.
[10] P. Maróti, C.A. Wraight, Flash-induced H^+-binding by bacterial photosynthetic reaction centers: influences of the redox states of the acceptor quinones and primary donor, Biochim. Biophys. Acta 934 (1988) 329–347.
[11] P.H. McPherson, M.Y. Okamura, G. Feher, Light-induced proton uptake by photosynthetic reaction centers from *Rhodobacter sphaeroides* R-26. I Protonation of the one-electron states $D^+Q_A^-$, DQ_A^-, $D^+Q_AQ_B^-$, and $DQ_AQ_B^-$, Biochim. Biophys. Acta 934 (1988) 348–368.
[12] Sebban, P. Maróti, D.K. Hanson, Electron and proton transfer to the quinones in bacterial photosynthetic reaction centers: insight from combined approaches of molecular genetics and biophysics, Biochimie 77 (1995) 677–694.
[13] J. Miksovska, M. Schiffer, D.K. Hanson, P. Sebban, Proton uptake by bacterial reaction centers: the protein complex responds in a similar manner to the reduction of either quinone acceptor, Proc. Natl. Acad. Sci. U. S. A. 96 (1999) 14348–14353.
[14] M.R. Gunner, B. Honig, Calculations of proton uptake in *Rhodobacter sphaeroides* reaction centers, in: J. Breton, A. Verméglio (Eds.), The Photosynthetic Bacterial Reaction Center II, Plenum Press, New York, 1992, pp. 403–410.
[15] P. Beroza, D.R. Fredkin, M.Y. Okamura, G. Feher, Electrostatic calculations of amino acid titration and electron transfer, $Q_A^-Q_B \rightarrow Q_AQ_B^-$, in the reaction center, Biophys. J. 68 (1995) 2233–2250.
[16] C.R.D. Lancaster, H. Michel, B. Honig, M.R. Gunner, Calculated coupling of electron and proton transfer in the photosynthetic reaction center of *Rhodopseudomonas viridis*, Biophys. J. 70 (1996) 2469–2492.
[17] B. Rabenstein, G.M. Ullmann, E.-W. Knapp, Calculation of protonation patterns in proteins with structural relaxation and molecular ensembles — application to the photosynthetic reaction center, Eur. Biophys. J. 27 (1998) 626–637.
[18] B. Rabenstein, G.M. Ullmann, E.-W. Knapp, Energetics of electron-transfer and protonation reactions of the quinones in the photosynthetic reaction center of *Rhodopseudomonas viridis*, Biochemistry 37 (1998) 2488–2495.
[19] E.G. Alexov, M.R. Gunner, Calculated protein and proton motions coupled to electron transfer: electron transfer from Q_A^- to Q_B in bacterial photosynthetic reaction centers, Biochemistry 38 (1999) 8253–8270.
[20] E. Alexov, J. Miksovska, L. Baciou, M. Schiffer, D.K. Hanson, P. Sebban, M.R. Gunner, Modeling the effects of mutations on the free energy of the first electron transfer from Q_A^- to Q_B in photosynthetic reaction centers, Biochemistry 39 (2000) 5940–5952.
[21] B. Rabenstein, G.M. Ullmann, E.-W. Knapp, Electron transfer between the quinones in the photosynthetic reaction center and its coupling to conformational changes, Biochemistry 39 (2000) 10487–10496.
[22] A.K. Grafton, R.A. Wheeler, Amino acid protonation states determine binding sites of the secondary ubiquinone and its anion in the *Rhodobacter sphaeroides* photosynthetic reaction center, J. Phys. Chem., B 103 (1999) 5380–5387.
[23] S.E. Walden, R.A. Wheeler, Protein conformational gate controlling binding site preference and migration for ubiquinone-B in the photosynthetic reaction center of *Rhodobacter sphaeroides*, J. Phys. Chem., B 106 (2002) 3001–3006.
[24] H. Ishikita, G. Morra, E.-W. Knapp, Redox potential of quinones in photosynthetic reaction centers from *Rhodobacter sphaeroides*: dependence on protonation of Glu-L212 and Asp-L213, Biochemistry 42 (2003) 3882–3892.
[25] H. Ishikita, A. Galstyan, E.-W. Knapp, Redox potential of the non-heme iron complex in bacterial photosynthetic reaction center, Biochim. Biophys. Acta 1767 (2007) 1300–1309.
[26] A. Taly, P. Sebban, J.C. Smith, G.M. Ullmann, The position of Q_B in the photosynthetic reaction center depends on pH: a theoretical analysis of the proton uptake upon Q_B reduction, Biophys. J. 84 (2003) 2090–2098.
[27] Z. Zhu, M.R. Gunner, Energetics of quinone-dependent electron and proton transfers in *Rhodobacter sphaeroides* photosynthetic reaction centers, Biochemistry 1 (2005) 82–96.

[28] P. Allen, G. Feher, T.O. Yeates, H. Komiya, D.C. Rees, Structure of the reaction center from *Rhodobacter sphaeroides* R-26: protein-cofactor (quinones and Fe^{2+}) interactions, Proc. Natl. Acad. Sci. U. S. A. 85 (1988) 8487–8491.

[29] O. El-Kabbani, C.-H. Chang, D. Tiede, J. Norris, M. Schiffer, Comparison of reaction centers from *Rhodobacter sphaeroides* and *Rhodopseudomonas viridis*: overall architecture and protein-pigment interactions, Biochemistry 30 (1991) 5361–5369.

[30] U. Ermler, G. Fritzsch, S.K. Buchanan, H. Michel, Structure of the photosynthetic reaction centre from *Rhodobacter sphaeroides* at 2.65 Å resolution: cofactors and protein-cofactor interactions, Structure 2 (1994) 925–936.

[31] A.J. Chirino, E.J. Lous, M. Huber, J.P. Allen, C.C. Schenck, M.L. Paddock, G. Feher, D. C. Rees, Crystallographic analyses of site-directed mutants of the photosynthetic reaction center from *Rhodobacter sphaeroides*, Biochemistry 33 (1994) 4584–4593.

[32] B. Arnoux, F. Reiss-Husson, Pigment-protein interactions in *Rhodobacter sphaeroides* Y photochemical reaction center; Comparison with other reaction center structures, Eur. Biophys. J. 24 (1996) 233–242.

[33] J. Deisenhofer, H. Michel, The photosynthetic reaction center from the purple bacterium *Rhodopseudomonas viridis*, EMBO J. 8 (1989) 2149–2170.

[34] C.R.D. Lancaster, U. Ermler, H. Michel, The structures of photosynthetic reaction centres from purple bacteria as revealed by X-ray crystallography, in: R.E. Blankenship, M.T. Madigan, C.E. Bauer (Eds.), Anoxygenic Photosynthetic Bacteria, Kluwer Academic Publishers, The Netherlands, 1995, pp. 503–526.

[35] C.R.D. Lancaster, H. Michel, The coupling of light-induced electron transfer and proton uptake as derived from crystal structures of reaction centres from *Rhodopseudomonas viridis* modified at the binding site of the secondary quinone, Q_B, Structure 5 (1997) 1339–1359.

[36] M.H.B. Stowell, T.M. McPhillips, D.C. Rees, S.M. Soltis, E. Abresch, G. Feher, Light-induced structural changes in photosynthetic reaction center: Implications for mechanism of electron-proton transfer, Science 276 (1997) 812–816.

[37] E.C. Abresch, M.L. Paddock, M.H.B. Stowell, T.M. McPhillips, H.L. Axelrod, S.M. Soltis, D.C. Rees, M.Y. Okamura, G. Feher, Identification of proton transfer pathways in the X-ray structure of the bacterial reaction center from *Rhodobacter sphaeroides*, Photosynth. Res. 55 (1998) 119–125.

[38] G. Fritzsch, J. Koepke, R. Diem, A. Kuglstatter, L. Baciou, Charge separation induces conformational changes in the photosynthetic reaction centre of purple bacteria, Acta Cryst. D58 (2002) 1660–1663.

[39] H. Ishikita, E.-W. Knapp, Variation of Ser-L223 hydrogen bonding with the Q_B redox state in reaction centers from *Rhodobacter sphaeroides*, J. Am. Chem. Soc. 126 (2004) 8059–8064.

[40] E. Nabedryk, M.L. Paddock, M.Y. Okamura, J. Breton, An isotope-edited FTIR investigation of the role of Ser-L223 in binding quinones (Q_B) and semiquinone (Q_B^-) in the reaction center from *Rhodobacter sphaeroides*, Biochemistry 44 (2005) 14519–14527.

[41] M.L. Paddock, M. Flores, R.A. Isaacson, C. Chang, E.C. Abresch, M.Y. Okamura, ENDOR spectroscopy reveals light induced movement of the H-bond from Ser-L223 upon forming the semiquinone Q_B^- reduction in reaction centers from *Rhodobacter sphaeroides*, Biochemistry 46 (2007) 8234–8243.

[42] K. Rothschild, FTIR difference spectroscopy of bacteriorhodopsin: toward a molecular model, J. Bioenerg. Biomembr. 24 (1992) 147–167.

[43] F. Siebert, Infrared spectroscopic investigations of retinal proteins, in: R.J.H. Clark, R.E. Hester (Eds.), Biomolecular Spectroscopy, Part A, John Wiley and Sons, New York, 1993, pp. 1–54.

[44] E. Nabedryk, J. Breton, R. Hienerwadel, C. Fogel, W. Mäntele, M.L. Paddock, M.Y. Okamura, Fourier transform infrared difference spectroscopy of secondary quinone acceptor photoreduction in proton transfer mutants of *Rhodobacter sphaeroides*, Biochemistry 34 (1995) 14722–14732.

[45] R.H. Hienerwadel, S. Grzybek, C. Fogel, W. Kreutz, M.Y. Okamura, M.L. Paddock, J. Breton, E. Nabedryk, W. Mäntele, Protonation of Glu-L212 following Q_B^- formation in the photosynthetic reaction center of *Rhodobacter sphaeroides*: evidence from time-resolved infrared spectroscopy, Biochemistry 34 (1995) 2832–2843.

[46] E. Nabedryk, J. Breton, M.Y. Okamura, M.L. Paddock, Simultaneous replacement of Asp-L210 and Asp-M17 with Asn increases proton uptake by Glu-L212 upon first electron transfer to Q_B in reaction centers from *Rhodobacter sphaeroides*, Biochemistry 40 (2001) 13826–13832.

[47] E. Nabedryk, J. Breton, M.Y. Okamura, M.L. Paddock, Proton uptake by carboxylic groups upon photoreduction of the secondary quinone (Q_B) in bacterial reaction centers from *Rhodobacter sphaeroides*: FTIR studies on the effects of replacing Glu H173, Biochemistry 37 (1998) 14457–14462.

[48] A. Mezzetti, E. Nabedryk, J. Breton, M.Y. Okamura, M.L. Paddock, G. Giacometti, W. Leibl, Rapid-scan Fourier transform infrared spectroscopy shows coupling of Glu-L212 protonation and electron transfer to Q_B in *Rhodobacter sphaeroides* reaction centers, Biochim. Biophys. Acta 1553 (2002) 320–330.

[49] E. Nabedryk, Characterization of the photoreduction of the secondary quinone Q_B in the photosynthetic reaction center from *Rhodobacter capsulatus* with FTIR spectroscopy, Biochim. Biophys. Acta 1411 (1999) 206–213.

[50] E. Nabedryk, J. Breton, H.M. Joshi, D.K. Hanson, Fourier transform infrared evidence of proton uptake by glutamate L212 upon reduction of the secondary quinone Q_B in the photosynthetic reaction center from *Rhodobacter capsulatus*, Biochemistry 39 (2000) 14654–14663.

[51] M.L. Paddock, S.H. Rongey, G. Feher, M.Y. Okamura, Pathway of proton transfer in bacterial reaction centers: replacement of glutamic acid 212 in the L subunit by glutamine inhibits quinone (secondary acceptor) turnover, Proc. Natl. Acad. Sci. U. S. A. 86 (1989) 6602–6606.

[52] E. Takahashi, C.A. Wraight, A crucial role for Asp^{L213} in the proton transfer pathway to the secondary quinone of reaction centers from *Rhodobacter sphaeroides*, Biochim. Biophys. Acta 1020 (1990) 107–111.

[53] E. Takahashi, C.A. Wraight, Proton and electron transfer in the acceptor quinone complex of *Rhodobacter sphaeroides* reaction centers: characterization of site-directed mutants of the two ionizable residues, Glu^{L212} and Asp^{L213}, in the Q_B binding site, Biochemistry 31 (1992) 855–866.

[54] M.L. Paddock, S.H. Rongey, P.H. McPherson, A. Juth, G. Feher, M.Y. Okamura, Pathway of proton transfer in bacterial reaction centers: role of aspartate-L213 in proton transfers associated with reduction of quinone to hydroquinone, Biochemistry 33 (1994) 734–745.

[55] P.H. McPherson, M. Schönfeld, M.L. Paddock, M.Y. Okamura, G. Feher, Protonation and free energy changes associated with formation of Q_BH_2 in native and Glu-L212→Gln mutant reaction centers from *Rhodobacter sphaeroides*, Biochemistry 33 (1994) 1181–1193.

[56] P. Maróti, D.K. Hanson, M. Schiffer, P. Sebban, Long-range electrostatic interaction in the bacterial photosynthetic reaction centre, Nat. Struct. Biol. 2 (1995) 1057–1059.

[57] J. Miksovska, L. Kálman, M. Schiffer, P. Maróti, P. Sebban, D.K. Hanson, In bacterial reaction centres rapid delivery to the second proton to Q_B can be achieved in the absence of Glu-L212, Biochemistry 36 (1997) 12216–12226.

[58] P. Brzezinski, M.L. Paddock, M.Y. Okamura, G. Feher, Light-induced electrogenic events associated with proton uptake upon forming Q_B^- in bacterial wild-type and mutant reaction centers, Biochim. Biophys. Acta 1321 (1997) 149–156.

[59] C.R.D. Lancaster, Ubiquinone reduction and protonation in photosynthetic reaction centers from *Rhodopseudomonas viridis*: X-ray structures and their functional implications, Biochim. Biophys. Acta 1365 (1998) 143–150.

[60] U. Zachariae, C.R.D. Lancaster, Proton uptake associated with the reduction of the primary quinone Q_A influences the binding site of the secondary quinone Q_B in *Rhodopseudomonas viridis* photosynthetic reaction center, Biochim. Biophys. Acta 1505 (2001) 280–290.

[61] O.A. Gopta, D.A. Bloch, D.A. Cherepanov, A.Y. Mulkidjanian, Temperature dependence of the electrogenic reaction in the Q_B site of the *Rhodobacter sphaeroides* photosynthetic reaction center: the $Q_A^-Q_B \rightarrow Q_AQ_B^-$ transition, FEBS Lett. 412 (1997) 490–494.

[62] A.Y. Mulkidjanian, Conformationally controlled p*K*-switching in membrane proteins: one more mechanism specific to the enzyme catalysis? FEBS Lett. 463 (1999) 199–204.

[63] D.A. Cherepanov, S.I. Bibikov, M.V. Bibikova, D.A. Bloch, L.A. Drachev, O.A. Gopta, D. Oesterhelt, A.Y. Semenov, A.Y. Mulkidjanian, Reduction and protonation of the secondary quinone acceptor of *Rhodobacter sphaeroides* photosynthetic reaction center: kinetic model based on a comparison of wild-type chromatophores with mutants carrying Arg→Ile substitution at sites 207 and 217 in the L-subunit, Biochim. Biophys. Acta 1459 (2000) 10–34.

[64] H. Cheap, J. Tandori, V. Derrien, M. Benoit, P. de Oliveira, J. Koepke, J. Lavergne, P. Maroti, P. Sebban, Evidence for delocalized anticooperative flash induced proton binding as revealed by mutants at the M266His iron ligand in bacterial reaction centers, Biochemistry 46 (2007) 4510–4521.

[65] J. Breton, C. Boullais, G. Berger, C. Mioskowski, E. Nabedryk, Binding-sites of quinones in photosynthetic bacterial reaction centers investigated by light-induced FTIR difference spectroscopy: symmetry of the carbonyl interactions and close equivalence of the Q_B vibrations in *Rhodobacter sphaeroides* and *Rhodopseudomonas viridis* probed by isotope labeling, Biochemistry 34 (1995) 11606–11616.

[66] R. Brudler, H.J.M. de Groot, W.B.S. van Liemt, P. Gast, A.J. Hoff, J. Lugtenburg, K. Gerwert, FTIR spectroscopy shows weak symmetric hydrogen bonding of the Q_B carbonyl groups in *Rhodobacter sphaeroides* R26 reaction centers, FEBS Lett. 370 (1995) 88–92.

[67] J. Breton, E. Nabedryk, Protein-quinone interactions in the bacterial photosynthetic reaction center: Light-induced FTIR difference spectroscopy of the quinone vibrations, Biochim. Biophys. Acta 1275 (1996) 84–90.

[68] J. Breton, C. Boullais, C. Mioskowski, P. Sebban, L. Baciou, E. Nabedryk, Vibrational spectroscopy favors a unique Q_B binding site at the proximal position in wild-type reaction centers and in the Pro-L209→Tyr mutant from *Rhodobacter sphaeroides*, Biochemistry 41 (2002) 12921–12927.

[69] J. Breton, M.C. Wakeham, P.K. Fyfe, Jones, E. Nabedryk, Characterization of bonding interactions of Q_B upon photoreduction via A-branch or B-branch electron transfer in mutant reaction centers from *Rhodobacter sphaeroides*, Biochim. Biophys. Acta 1656 (2004) 127–138.

[70] J. Breton, Absence of large-scale displacement of quinone Q_B in bacterial photosynthetic reaction centers, Biochemistry 43 (2004) 3318–3326.

[71] E. Nabedryk, J. Breton, P. Sebban, L. Baciou, Quinone (Q_B) binding site and protein structural changes in photosynthetic reaction center mutants at Pro-L209 revealed by vibrational spectroscopy, Biochemistry 42 (2003) 5819–5827.

[72] D. Kleinfeld, M.Y. Okamura, G. Feher, Electron-transfer kinetics in photosynthetic reaction centers cooled to cryogenic temperatures in the charge-separated state: evidence for light-induced structural changes, Biochemistry 23 (1984) 5780–5786.

[73] Q. Xu, M.R. Gunner, Trapping conformational intermediate states in the reaction center protein from photosynthetic bacteria, Biochemistry 40 (2001) 3232–3241.

[74] L.M. Utschig, M.C. Thurnauer, D.M. Tiede, O.G. Poluektov, Low-temperature interquinone electron transfer in photosynthetic reaction centers from *Rhodobacter sphaeroides* and *Blastochloris viridis*: characterization of Q_B^- states by high-frequency electron paramagnetic resonance (EPR) and electron-nuclear double resonance (ENDOR), Biochemistry 44 (2005) 14131–14142.

[75] P.R. Pokkuluri, P.D. Laible, A.E. Crawford, J.F. Mayfield, M.A. Yousef, S.L. Ginell, D.K. Hanson, M. Schiffer, Temperature and cryoprotectant influence secondary quinone binding position in bacterial reaction centers, FEBS Lett. 570 (2004) 171–174.

[76] W. Mäntele, Reaction-induced infrared difference spectroscopy for the study of protein function and reaction mechanisms, Trends Biochem. Sci. 18 (1993) 197–202.

[77] E. Nabedryk, Light-induced Fourier transform infrared difference spectroscopy of the primary electron donor in photosynthetic reaction centers, in: H.H. Mantsch, D. Chapman (Eds.), Infrared Spectroscopy of Biomolecules, Wiley-Liss, New York, 1996, pp. 39–81.

[78] R. Vogel, F. Siebert, Vibrational spectroscopy as a tool for probing protein function, Curr. Opin. Chem. Biol. 4 (2000) 518–523.

[79] C. Berthomieu, R. Hienerwadel, Vibrational spectroscopy to study the properties of redox-active tyrosines in photosystem II and other proteins, Biochim. Biophys. Acta 1707 (2004) 51–66.

[80] M. Lutz, W. Mäntele, Vibrational spectroscopy of chlorophylls, in: H. Scheer (Ed.), The Chlorophylls, CRC Press, 1991, pp. 855–902.

[81] J.-R. Burie, C. Boullais, M. Nonella, C. Mioskowski, E. Nabedryk, J. Breton, Importance of the conformation of methoxy groups on the vibrational and electrochemical properties of ubiquinones, J. Phys. Chem., B 101 (1997) 6607–6617.

[82] J. Breton, C. Boullais, J.-R. Burie, E. Nabedryk, C. Mioskowski, Binding-sites of quinones in photosynthetic bacterial reaction centers investigated by light-induced FTIR difference spectroscopy: assignment of the interactions of each carbonyl of Q_A in *Rhodobacter sphaeroides* using site-specific ^{13}C-labeled ubiquinone, Biochemistry 33 (1994) 14378–14386.

[83] R. Brudler, H.J.M. de Groot, W.B.S. van Liemt, W.F. Steggerda, R. Esmeijer, P. Gast, A.J. Hoff, J. Lugtenburg, K. Gerwert, Asymmetric binding of the 1-and 4-C=O groups of Q_A in *Rhodobacter sphaeroides* R26 reaction centers monitored by Fourier transform infra-red spectroscopy using site-specific isotopically labelled ubiquinone-10, EMBO J. 13 (1994) 5523–5530.

[84] J. Breton, J. Lavergne, M.C. Wakeham, E. Nabedryk, M.R. Jones, The unusually strong hydrogen bond between the carbonyl of Q_A and His M219 in the *Rhodobacter sphaeroides* reaction center is not essential for efficient electron transfer from Q_A^- to Q_B, Biochemistry 46 (2007) 6468–6476.

[85] K.E. McAuley, P.K. Fyfe, J.P. Ridge, R.J. Cogdell, N.W. Isaacs, M.R. Jones, Ubiquinone binding, ubiquinone exclusion, and detailed cofactor conformation in a mutant bacterial reaction center, Biochemistry 49 (2000) 15032–15043.

[86] A. Kuglstatter, U. Ermler, H. Michel, L. Baciou, G. Fritzsch, X-ray structure analyses of photosynthetic reaction center variants from *Rhodobacter sphaeroides*: structural changes induced by point mutations at position L209 modulate electron and proton transfer, Biochemistry 40 (2001) 4253–4260.

[87] P.R. Pokkuluri, P.D. Laible, Y.-L. Deng, T.N. Wong, D.K. Hanson, M. Schiffer, The structure of a mutant photosynthetic reaction center shows unexpected changes in main chain orientations and quinone position, Biochemistry 41 (2002) 5998–6007.

[88] L. Baciou, H. Michel, Interruption of the water chain in the reaction center from *Rhodobacter sphaeroides* reduces the rates of the proton uptake and of the second electron transfer to Q_B, Biochemistry 34 (1995) 7967–7972.

[89] J. Tandori, P. Sebban, H. Michel, L. Baciou, *Rhodobacter sphaeroides* reaction centers: mutation of proline M209 to aromatic residues in the vicinity of a water channel alters the dynamic coupling between electron and proton transfer processes, Biochemistry 38 (1999) 13179–13187.

[90] Q. Xu, L. Baciou, P. Sebban, M.R. Gunner, Exploring the energy landscape for Q_A^- to Q_B electron transfer in photosynthetic reaction centers: effect of substrate position and tail length on the conformational gating step, Biochemistry 41 (2002) 10021–10025.

[91] J.P. Ridge, M.E. van Brederode, M.G. Goodwin, R. van Grondelle, M.R. Jones, Mutations that modify or exclude binding of the Q_A ubiquinone and carotenoid in the reaction center from *Rhodobacter sphaeroides*, Photosynth. Res. 59 (1999) 9–26.

[92] M.C. Wakeham, M.G. Goodwin, C. McKibbin, M.R. Jones, Photo-accumulation of the $P^+Q_B^-$ radical pair state in purple bacterial reaction centres that lack the Q_A ubiquinone, FEBS Lett. 540 (2003) 234–240.

[93] M.C. Wakeham, J. Breton, E. Nabedryk, M.R. Jones, Formation of a semiquinone at the Q_B site by A-branch or B-branch electron transfer in the reaction centre from *Rhodobacter sphaeroides*, Biochemistry 43 (2004) 4755–4763.

[94] D.K. Hanson, L. Baciou, D.M. Tiede, S.L. Nance, M. Schiffer, P. Sebban, In bacterial reaction centers protons can diffuse to the secondary quinone by alternative pathways, Biochim. Biophys. Acta 1102 (1992) 260–265.

[95] R.H.G. Baxter, B.-L. Seagle, N. Ponomarenko, J.R. Norris, Specific radiation damage illustrates light-induced structural changes in the photosynthetic reaction center, J. Am. Chem. Soc. 126 (2004) 16728–16729.

[96] R.H.G. Baxter, B.-L. Seagle, N. Ponomarenko, V. Srajer, R. Pahl, K. Moffat, J.R. Norris, Cryogenic structure of in the photosynthetic reaction center of *Blastochloris viridis* in the light and in the dark, Acta Cryst. D61 (2005) 605–612.

[97] M.L. Paddock, C. Chang, Q. Xu, E.C. Abresch, H.L. Axelrod, G. Feher, M.Y. Okamura, Quinone (Q_B) reduction by B-branch electron transfer in mutant bacterial reaction centers from *Rb. sphaeroides*: quantum efficiency and X-ray structure, Biochemistry 44 (2005) 6920–6928.

[98] Q. Xu, H.L. Axelrod, E.C. Abresch, M.L. Paddock, M.Y. Okamura, G. Feher, X-ray structure determination of three mutants of the bacterial photosynthetic reaction center from *Rb. sphaeroides*: altered proton transfer pathways, Structure 12 (2004) 703–715.

[99] A. Verméglio, Secondary electron transfer in reaction centers of *Rhodopseudomonas sphaeroides*. Out-of-phase periodicity of two for the formation of ubisemiquinone and fully reduced ubiquinone, Biochim. Biophys. Acta 459 (1977) 516–524.

[100] C.A. Wraight, Electron acceptors of photosynthetic bacterial reaction centers. Direct observation of oscillatory behaviour suggesting two closely equivalent ubiquinones, Biochim. Biophys. Acta 459 (1977) 525–531.

[101] J. Breton, C. Berthomieu, D.L. Thibodeau, E. Nabedryk, Probing the secondary quinone (Q_B) environment in photosynthetic bacterial reaction centers by light-induced FTIR difference spectroscopy, FEBS Lett. 288 (1991) 109–113.

[102] A. Mezzetti, W. Leibl, J. Breton, E. Nabedryk, Photoreduction of the quinone pool in the bacterial photosynthetic membrane: identification of infrared marker bands for quinol formation, FEBS Lett. 537 (2003) 161–165.

[103] H.L. Axelrod, E.C. Abresch, M.L. Paddock, M.Y. Okamura, G. Feher, Determination of the binding sites of the proton transfer inhibitors Cd^{2+} and Zn^{2+} in bacterial reaction centers, Proc. Natl. Acad. Sci. U. S. A. 97 (2000) 1542–1547.

[104] R.H.G. Baxter, N. Ponomarenko, V. Srajer, R. Pahl, K. Moffat, J.R. Norris, Time-resolved crystallographic studies of light-induced structural changes in the photosynthetic reaction center, Proc. Natl. Acad. Sci. U. S. A. 101 (2004) 5982–5987.

[105] M.L. Paddock, M. Flores, R.A. Isaacson, C. Chang, E.C. Abresch, P. Selvaduray, M.Y. Okamura, Trapped conformational states of semiquinone ($D^+Q_B^-$) formed by B-branch electron transfer at low temperature in *Rhodobacter sphaeroides* reaction centers, Biochemistry 46 (2006) 14032–14042.

[106] Q. Xu, M.R. Gunner, Exploring the energy profile of the Q_A^- to Q_B electron transfer in photosynthetic reaction centers: pH dependence of the conformational gating step, Biochemistry 41 (2002) 2694–2701.

[107] J.C. McComb, R.R. Stein, C.A. Wraight, Investigations on the influence of headgroup substitution and isoprene side-chain length in the function of primary and secondary quinones of bacterial reaction centers, Biochim. Biophys. Acta 1015 (1990) 156–171.

[108] P. Ädelroth, M.L. Paddock, L.B. Sagle, G. Feher, M.Y. Okamura, Identification of the proton pathway in bacterial reaction centers: both protons associated with reduction of Q_B to Q_BH_2 share a common entry point, Proc. Natl. Acad. Sci. U. S. A. 97 (2000) 13086–13091.

[109] M.L. Paddock, P.H. McPherson, G. Feher, M.Y. Okamura, Pathway of proton transfer in bacterial reaction centers: replacement of serine-L223 by alanine inhibits electron and proton transfers associated with reduction of quinone to hydroquinone, Proc. Natl. Acad. Sci. U. S. A. 87 (1990) 6803–6807.

[110] M.L. Paddock, G. Feher, M.Y. Okamura, Pathway of proton transfer in bacterial reaction centers: further investigations on the role of Ser-L223 studied by site-directed mutagenesis, Biochemistry 34 (1995) 15742–15750.

[111] M.L. Paddock, S.H. Rongey, E.C. Abresch, G. Feher, M.Y. Okamura, Reaction centers from three herbicide-resistant mutants of *Rhodobacter sphaeroides* 2.4.1: sequence analysis and preliminary characterization, Photosynth. Res. 17 (1988) 75–96.

[112] W. Leibl, I. Sinning, G. Ewald, H. Michel, J. Breton, Evidence that Ser-L223 is involved in the proton transfer pathway to Q_B in the photosynthetic reaction center of *Rhodopseudomonas viridis*, Biochemistry 32 (1993) 1958–1964.

[113] S.I. Bibikov, D.A. Bloch, A. Cherepanov, D. Oesterhelt, A.Yu. Semenov, Flash-induced electrogenic reactions in the SA(L223) reaction center mutant in *Rhodobacter sphaeroides* chromatophores, FEBS Lett. 341 (1994) 10–14.

[114] E. Nabedryk, J. Breton, R. Hienerwadel, C. Fogel, W. Mäntele, M.L. Paddock, M.Y. Okamura, FTIR spectroscopy of Q_B photoreduction in *Rhodobacter sphaeroides* reaction centers: effects of site-directed replacements at Glu L212, Asp L213, Asp L210, and of $^1H/^2H$ exchange, in: P. Mathis (Ed.), Photosynthesis: from Light to Biosphere, vol. I, Kluwer Academic Publishers, The Netherlands, 1995, pp. 875–878.

[115] P. Maróti, C.A. Wraight, Flash-induced H^+ binding by bacterial photosynthetic reaction centers: comparison of spectrophotometric and conductimetric methods, Biochim. Biophys. Acta 934 (1988) 314–328.

[116] P. Maróti, Flash-induced proton transfer in photosynthetic bacteria, Photosynth. Res. (1993) 1–17.

[117] P. Ädelroth, M.L. Paddock, A. Tehrani, J.T. Beatty, G. Feher, M.Y. Okamura, Identification of the proton pathway in bacterial reaction centers: decrease of proton transfer rate by mutation of surface histidines at H126 and H128 and chemical rescue by imidazole identifies the initial proton donors, Biochemistry 48 (2001) 14538–14546.

[118] D.K. Hanson, S.L. Nance, M. Schiffer, Second-site mutation at M43 (Asn→Asp) compensates for the loss of two acidic residues in the Q_B site of the reaction center, Photosynth. Res. 32 (1992) 147–153.

[119] S.H. Rongey, M.L. Paddock, G. Feher, M.Y. Okamura, Pathway of proton transfer in bacterial reaction centers: second-site mutation Asn-M44→Asp restores electron and proton transfer in reaction centers from the photosynthetically deficient Asp-L213→Asn mutant of *Rhodobacter sphaeroides*, Proc. Natl. Acad. Sci. U. S. A. 90 (1993) 1325–1329.

[120] P. Sebban, P. Maróti, M. Schiffer, D.K. Hanson, Electrostatic dominoes: long distance propagation of mutational effects in photosynthetic reaction centers of *Rhodobacter capsulatus*, Biochemistry 34 (1995) 8390–8397.

[121] J. Tandori, L. Baciou, E. Alexov, P. Maróti, M. Schiffer, D.K. Hanson, P. Sebban, Revealing the involvement of extended hydrogen bond networks in the cooperative function between distant sites in bacterial reaction centers, J. Biol. Chem. 276 (2001) 45513–45515.

[122] J. Tandori, P. Maróti, E. Alexov, P. Sebban, L. Baciou, Key role of proline L209 in connecting the distant quinone pockets in the reaction center of *Rhodobacter sphaeroides*, Proc. Natl. Acad. Sci. U. S. A. 99 (2002) 6702–6706.

[123] H. Ishikita, E.-W. Knapp, Energetics of proton transfer pathways in reaction centers from *Rhodobacter sphaeroides* The Glu-H173 activated mutants, J. Biol. Chem. 280 (2005) 12446–12450.

[124] C. Cometta-Morini, C. Scharnagl, S.F. Fischer, Proton transfer to ubiquinone Q_B in the photosynthetic reaction center of *Rps. viridis*: the role of electrostatic interactions, Int. J. Quantum Chem.: Quantum Biology Symposium, vol.20, John Wiley and Sons, Inc., 1993, pp. 89–106.

[125] J. Breton, E. Nabedryk, C. Mioskowski, C. Boullais, Protein-quinone interactions in photosynthetic bacterial reaction centers investigated by light-induced FTIR

difference spectroscopy, in: M.-E. Michel-Beyerle (Ed.), The Reaction Center of Photosynthetic Bacteria, Structure and Dynamics, Springer-Verlag, New York, 1996, pp. 381–394.
[126] J. Breton, E. Nabedryk, Proton uptake upon quinone reduction in bacterial reaction centers: IR signature and possible participation of a highly polarizable hydrogen bond network, Photosynth. Res. 55 (1998) 301–307.
[127] J. Breton, M. Bibikova, D. Oesterhelt, E. Nabedryk, Electrostatic influence of Q_A or Q_B reduction on the 10a-ester C=O vibration of H_A in *Rp. viridis*, in: G. Garab (Ed.), Photosynthesis: Mechanisms and Effects, vol. 2, Kluwer Academic Publishers, Dordrecht, 1998, pp. 687–692.
[128] L.J. Bellamy, The infrared spectra of complexed molecules, Chapman & Hall, London, 1975.
[129] A.K. Dioumaev, M.S. Braiman, Modeling vibrational spectra of amino acid side chains in proteins: the carbonyl stretch frequency of buried carboxylic residues, J. Am. Chem. Soc. 117 (1995) 10572–10574.
[130] P.R. Rich, M. Iwaki, Infrared spectroscopy as a tool to study protonation reactions within proteins, in: M. Wikstrom (Ed.), Biophysical and Structural Aspects of Bioenergetics, Royal Society of Chemistry, Cambridge, 2005, pp. 314–333., Chap. 13.
[131] K. Gerwert, B. Hess, J. Soppa, D. Oesterhelt, Role of aspartate-96 in proton translocation by bacteriorhodopsin, Proc. Natl. Acad. Sci. U. S. A. 86 (1989) 4943–4947.
[132] M.S. Braiman, O. Bousché, K.J. Rothschild, Protein dynamics in the bacteriorhodopsin photocycle: submillisecond fourier transform infrared spectra of the L, M, and N photointermediates, Proc. Natl. Acad. Sci. U. S. A. 88 (1991) 2388–2392.
[133] K. Fahmy, F. Jager, M. Beck, T.A. Zvyaga, T.P. Sakmar, F. Siebert, Protonation states of membrane-embedded carboxylic acid groups in rhodopsin and metarhodopsin II: a Fourier-transform infrared spectroscopy study of site-directed mutants, Proc. Natl. Acad. Sci. U. S. A. 90 (1993) 10206–10210.
[134] W. Mäntele, E. Nabedryk, B.A. Tavitian, J. Breton, Light-induced Fourier transform infrared (FTIR) spectroscopic investigations of the primary donor oxidation in bacterial photosynthesis, FEBS Lett. 187 (1985) 227–232.
[135] W.G. Mäntele, A.M. Wollenweber, E. Nabedryk, J. Breton, Infrared spectroelectrochemistry of bacteriochlorophylls and bacteriopheophytins: implications for the binding of the pigments in the reaction center from photosynthetic bacteria, Proc. Natl. Acad. Sci. U. S. A. 85 (1988) 8468–8472.
[136] E. Nabedryk, W. Mäntele, B. Tavitian, J. Breton, Light-induced Fourier transform infrared (FTIR) spectroscopic investigations of the intermediary electron acceptor reduction in bacterial photosynthesis, Photochem. Photobiol. 43 (1986) 461–465.
[137] E. Nabedryk, K.A. Bagley, D.L. Thibodeau, M. Bauscher, W. Mäntele, J. Breton, A protein conformational change associated with the photoreduction of the primary and secondary quinones in the bacterial reaction center, Biochim. Biophys. Acta 266 (1990) 59–62.
[138] D. Moss, E. Nabedryk, J. Breton, W. Mäntele, Redox-linked conformational changes in proteins detected by a combination of infrared spectroscopy and protein electrochemistry, Eur. J. Biochem. 187 (1990) 565–572.
[139] M. Bauscher, E. Nabedryk, K. Bagley, J. Breton, W. Mäntele, Investigation of models for photosynthetic electron acceptors: infrared spectroelectrochemistry of ubiquinone and its anions, FEBS Lett. 261 (1990) 191–195.
[140] M. Bauscher, W. Mäntele, Electrochemical and infrared-spectroscopic characterization of redox reactions of *p*-quinones, J. Phys. Chem. 96 (1992) 11101–11108.
[141] Yu.N. Chirgadze, O.V. Fedorov, N.P. Trushina, Estimation of amino acid residue side-chain absorption in the infrared spectra of protein solutions in heavy water, Biopolymers 14 (1975) 679–694.
[142] S.Yu. Venyaminov, N.N. Kalnin, Quantitative IR spectrophotometry of peptide compounds in water (H_2O) solutions. I. Spectral parameters of amino acid residue absorption bands, Biopolymers 30 (1990) 1243–1257.
[143] K. Rahmelow, W. Hübner, Th. Ackermann, Infrared absorbance of protein side chains, Anal. Biochem. 257 (1998) 1–11.
[144] E. Nabedryk, J. Breton, M.Y. Okamura, M.L. Paddock, Protonation of carboxylic acid groups in *Rb. sphaeroides* reaction centers upon Q_B reduction: effect of interchanging Glu and Asp at the L213 and L212 sites, in: G. Garab (Ed.), Photosynthesis: Mechanisms and Effects, vol. 2, Kluwer Academic Publishers, Dordrecht, The Netherlands, 1998, pp. 845–848.
[145] J. Breton, Steady-state FTIR spectra of the photoreduction of Q_A and Q_B in *Rhodobacter sphaeroides* reaction centers provide evidence against the presence of a proposed transient electron acceptor X between the two quinones, Biochemistry 46 (2007) 4459–4465.
[146] E. Nabedryk, J. Breton, M.Y. Okamura, M.L. Paddock, Identification of a novel protonation pattern for carboxylic acids upon Q_B photoreduction in *Rhodobacter sphaeroides* reaction center mutants at Asp-L213 and Glu-L212 sites, Biochemistry 43 (2004) 7236–7243.
[147] E. Nabedryk, M.L. Paddock, M.Y. Okamura, J. Breton, Monitoring the pH dependence of IR carboxylic acid signals upon Q_B^- formation in the Glu-L212 Asp/Asp-L213 Glu swap mutant reaction center from *Rhodobacter sphaeroides*, Biochemistry 46 (2007) 1176–1182.
[148] S. Hermes, J.M. Stachnik, D. Onidas, A. Remy, E. Hofmann, K. Gerwert, Proton uptake in the reaction center mutant L210DN from *Rhodobacter sphaeroides* via protonated water molecules, Biochemistry 45 (2006) 13741–13749.
[149] M.L. Paddock, G. Feher, M.Y. Okamura, Identification of the proton pathway in bacterial reaction centers: replacement of Asp-M17 and Asp-L210 with Asn reduces the proton transfer rate in the presence of Cd^{2+}, Proc. Natl. Acad. U. S. A. 97 (2000) 1548–1553.
[150] M.L. Paddock, P. Ädelroth, C. Chang, E.C. Abresch, G. Feher, M.Y. Okamura, Identification of the proton pathway in bacterial reaction centers: cooperation between Asp-M17 and Asp-L210 facilitates proton transfer to the secondary quinone (Q_B), Biochemistry 40 (2001) 6893–6902.
[151] E. Takahashi, C.A. Wraight, Potentiation of proton transfer function by electrostatic interactions in photosynthetic reaction centers from *Rhodobacter sphaeroides*: first results from site-directed mutation of the H subunit, Proc. Natl. Acad. U. S. A. 93 (1996) 2640–2645.
[152] R. Hienerwadel, D. Thibodeau, F. Lenz, E. Nabedryk, J. Breton, W. Kreutz, W. Maentele, Time-resolved infrared spectroscopy of electron transfer in bacterial photosynthetic reaction centers: dynamics of binding and interaction upon Q_A and Q_B reduction, Biochemistry 31 (1992) 5799–5808.
[153] R. Hienerwadel, E. Nabedryk, M.L. Paddock, S. Rongey, M.Y. Okamura, W. Maentele, J. Breton, Proton transfer mutants of *Rb. sphaeroides*: characterization of reaction centers by infrared spectroscopy, in: N. Murata (Ed.), Research in Photosynthesis, vol. I, Kluwer Academic Publishers, The Netherlands, 1992, pp. 440–447.
[154] E. Nabedryk, J. Breton, M.Y. Okamura, M.L. Paddock, Direct evidence of structural changes in reaction centers of *Rb. sphaeroides* containing suppressor mutations for Asp→L213 Asn: a FTIR study of Q_B reduction, Photosynth. Res. 55 (1998) 293–299.
[155] M.L. Paddock, G. Feher, M.Y. Okamura, Proton and electron transfer to the secondary quinone (Q_B) in bacterial reaction centers: the effect of interchanging the electrostatics in the vicinity of Q_B by interchanging Asp and Glu at the L212 and L213 sites, Biochemistry 36 (1997) 14238–14249.
[156] C. Fogel, S. Grzybek, R. Hienerwadel, M.Y. Okamura, M.L. Paddock, J. Breton, E. Nabedryk, W. Maentele, Time-resolved infrared and steady-state Fourier transform infrared spectroscopy of native and mutant reaction centers of *Rb. sphaeroides*, in: P. Mathis (Ed.), Photosynthesis: from Light to Biosphere, vol. I, Kluwer Academic Publishers, The Netherlands, 1995, pp. 591–594.
[157] E. Nabedryk, J. Breton, R. Hienerwadel, W. Mäntele, M.L. Paddock, S.H. Rongey, G. Feher, M.Y. Okamura, Light-induced FTIR difference spectroscopy of proton transfer mutants of *Rb. sphaeroides*, Biophys. J. 64 (1993) A214.
[158] D.L. Thibodeau, E. Nabedryk, R. Hienerwadel, F. Lenz, W. Mäntele, J. Breton, Time-resolved FTIR spectroscopy of quinones in *Rb. sphaeroides* reaction centers, Biochim. Biophys. Acta 1020 (1990) 253–259.
[159] R. Brudler, K. Gerwert, Step-scan FTIR spectroscopy resolves the $Q_A^-Q_B \rightarrow Q_AQ_B^-$ transition in *Rb. sphaeroides* R26 reaction centres, Photosynth. Res. 55 (1998) 261–266.
[160] A.J. Watson, P.K. Fyfe, D.F. Frolov, M.C. Wakeham, E. Nabedryk, R. van Grondelle, J. Breton, M.R. Jones, Replacement or exclusion of the B-branch bacteriopheophytin in the purple bacterial reaction centre: the H_B cofactor is not required for assembly or core function of the *Rhodobacter sphaeroides* complex, Biochim. Biophys. Acta 1710 (2005) 34–46.
[161] G. Fritzsch, L. Kampmann, G. Kapaun, H. Michel, Water clusters in the reaction center of *Rb. sphaeroides*, Photosynth. Res. 55 (1998) 127–132.
[162] V.Z. Spassov, H. Lueke, K. Gerwert, D. Bashford, pK(a) Calculations suggest storage of an excess proton in a hydrogen-bonded water network in bacteriorhodopsin, J. Mol. Biol. 312 (2001) 203–219.
[163] F. Garczarek, J. Wang, M.A. El-Sayed, K. Gerwert, The assignment of the different infrared continuum absorbance changes observed in the 3000–1800 cm^{-1} region during the bacteriorhodopsin photocycle, Biophys. J. 87 (2004) 2676–2682.
[164] F. Garczarek, L.S. Brown, J.K. Lanyi, K. Gerwert, Proton binding within a membrane protein by a protonated water cluster, Proc. Natl. Acad. Sci. U. S. A. 102 (2005) 3633–3638.
[165] F. Garczarek, K. Gerwert, Functional waters in intraprotein proton transfer monitored by FTIR difference spectroscopy, Nature 439 (2006) 109–112.
[166] G. Zundel, Proton transfer in and protein polarizability of hydrogen bonds: IR and theoretical studies regarding mechanisms in biological systems, J. Mol. Struct. 177 (1988) 43–68.
[167] G. Zundel, Hydrogen bonds with large proton polarizability and proton transfer processes in electrochemistry and biology, in: I. Prigogine, S.A. Rice (Eds.), Adv. Chem. Phys, vol. 111, John Wiley & Sons, 2000, pp. 1–217.
[168] R. Pomès, B. Roux, Free energy profiles for H^+conduction along hydrogen bonded chains of water molecules, Biophys. J. 75 (1998) 33–40.
[169] R. Vuilleumier, D. Borgis, An extended empirical valence bond model for describing proton mobility in water, Isr. J. Chem. 39 (1999) 457–467.
[170] D. Marx, M.E. Tuckerman, J. Hutter, M. Parrinello, The nature of the hydrated excess proton in water, Nature 397 (1999) 601–604.
[171] T.J.F. Day, U.W. Schmitt, G.A. Voth, The mechanism of hydrated proton transport in water, J. Am. Chem Soc. 122 (2000) 12027–12028.
[172] J.M. Headrick, E.G. Diken, R.S. Walters, N.I. Hammer, R.A. Christie, J. Cui, E.M. Myshakin, M.A. Duncan, M.A. Johnson, K.D. Jordan, Spectral signatures of hydrated proton vibrations in water clusters, Science 308 (2005) 1765–1769.
[173] E. Nabedryk, M.Y. Okamura, M.L. Paddock, J. Breton, Perturbation of the polarizable proton infrared continuum upon Q_B reduction in mutant reaction centers from *Rb. sphaeroides*, Biophys. J. 82 (2002) 197a.
[174] U. Heinen, L.M. Utschig, O.G. Poluektov, G. Link, E. Ohmes, G. Kothe, Structure of the charge separated $P^+_{865}Q_A^-$ in the photosynthetic reaction centers of *Rb. sphaeroide* by quantum beat oscillations and high-field electron paramagnetic resonance: evidence for light-induced reorientation, J. Am. Chem. Soc. 129 (2007) 15935–15946.
[175] V.A. Lórenz-Fonfria, Y. Furutani, H. Kandori, Active internal waters in the bacteriorhodopsin photocycle. A comparative study of the L and M intermediates at room and cryogenic temperatures by infrared spectroscopy, Biochemistry 47 (2008) 4071–4081.